APR 20 1966
FEB 8 1967
APR 1 1968
DEC 31 1974
MAY 8 1979

CATALOGED BY DDC
AS AD No. 58088

U. S. NAVAL ORDNANCE LABORATORY
White Oak, Silver Spring 19, Maryland

NAVAL ORDNANCE LABORATORY MEMORANDUM 10594

4 April 1950

From: J. C. Crown and W. H. Heybey
To: NOL Files
Via: Chief, Hyperballistics Division
Aeroballistic Research Department

Subj: Supersonic Nozzle Design. (Project NOL 159)

Abstract: The theory of supersonic flow in nozzles is discussed, emphasis being placed on the physical rather than the mathematical point of view. Methods, both graphic and analytic, for designing nozzles are described together with a discussion of design factors. In addition, the analysis of given nozzle shapes to determine velocity distribution and possible existence of shock waves is considered. A description of a supersonic protractor is included in conjunction with a discussion of its application to nozzle analysis and design. The correction of nozzle contours for boundary layer and other errors is also discussed.

AEDC TECHNICAL LIBRARY
5 0720 00045 3680

Foreword: The material presented herein was obtained from NACA TN 1651 by J. C. Crown and NOLM 9132 by W. Heybey. Certain extra material has been added and these are being published together for the use of the NOL personnel. They also constitute the subject matter of a course on nozzle design given by the authors. This report does not necessarily represent the final opinion of the Laboratory.

This document is supplied for use in connection with and for the duration of a specific contract unless circumstances warrant earlier recall. However, as soon as it serves its purpose you will help reduce our reproduction cost by returning it to:
ARMED SERVICES TECHNICAL INFORMATION AGENCY
DOCUMENT SERVICE CENTER
Knott Building, Dayton 2, Ohio

(a) Busemann, A. Gasdynamik. Handbuch der Experimentalphysik, Akademische Verlagsgesellschaft, Leipzig. Bd. 4, Teil 1, 1931, S. 341-460.
(b) Preiswerk, Ernst. Application to the Methods of Gas Dynamics to Water Flows with Free Surface. Part I. Flows With No Energy Dissipation. NACA TM No. 934 (1940).
(c) Foelsch, Kuno. A New Method of Designing Two-Dimensional Laval Nozzles for a Parallel and Uniform Jet. North American Aviation Report No. NA-46-235 (Mar. 1946).
(d) Shapiro, A. H. "Nozzles for Supersonic Flow Without Shock Fronts." Jour. Appld. Mech., 11, No. 2, A-93-A-100 (1944).
(e) Liepmann, Hans W., and Puckett, Allen E. Introduction to Aerodynamics of a Compressible Fluid. John Wiley and Sons, Inc. (1947).

Per TAB 74-22, Dtd 25 OCT, 1974

(f) Taylor, G. I. and Maccoll, J. W. "The Mechanics of Compressible Fluids. Two-Dimensional Flow at Supersonic Speeds." Aerodynamic Theory, III, H, Ch. IV, W. F. Durand, Julius Springer (Berlin), 23-249 (1935).
(g) Puckett, Allen E. "Supersonic Nozzle Design." Jour. Appld. Mech., 13, No. 4, A-265-A-270 (1946).
(h) Shapiro, Ascher H. and Edelman, Gilbert M. "Method of Characteristics for Two-Dimensional Supersonic Flow - Graphical and Numerical Procedures." Jour. of Appld. Mech., 14, No. 2, A-154 - A-162 (1947).
(i) Temple, G. The Method of Characteristics in Supersonic Flow. British Rep. No. S.M.E. 3282, R.A.E. (1944).
(j) Puckett Allen E. Final Report on the Model Supersonic Wind-Tunnel Project. NDRC, Div. 2, Armor and Ordnance Rep. A-269. (Office of Scientific Research and Development) Rep. 3569 (1944).
(k) Eaton, A. R., and Deacon, P. O. Report on Pressure Calibration of M = 1.7(5) Nozzle, Lone Star Laboratory, Daingerfield, Texas, Page 8, JHU/APL/CM-374.

Encl: (A) Figures 1-25
(B) Tables I-II

I. Introduction

1. One of the major problems in the design of a supersonic wind tunnel is the determination of the contours of the supersonic nozzle so that parallel and uniform flow in the test section may be assured. Consequently, it is not surprising that the literature contains numerous papers on the subject of supersonic nozzle design. These vary widely in their degree of complexity and general availability. It is the purpose of this report to discuss these various methods and to present a guide for nozzle design. Only two-dimensional nozzles will be considered.

2. The most prominent method for determining nozzle contours is, perhaps, that of Prandtl and Buseman (reference a). The usual presentation of their method of characteristics is rather mathematical in nature. (See, e.g., Preiswerk, reference b). In order to provide the designer with a clearer physical picture of the flow in a nozzle, a different interpretation of the Prandtl-Buseman method is presented. The diverse systems for constructing nozzle shapes by this method are also presented, together with certain ramifications and supplementary useful information.

3. The Foelsch method (reference c) is included because its analytic nature offers certain advantages. These will be discussed later. Shapiro (reference d) has still another approach to the problem. His method, due to its approximate nature and because it has no special advantages, will not be considered.

II. Basic Theory

4. It is well known that, in a purely converging flow, the maximum uniform velocity that can be achieved across any section is that corresponding to the local velocity of sound. Further increases in velocity can be obtained only by subsequent expansion of the stream.

5. The essential and relevant features of a channel designed to produce supersonic flow are shown in Figure 1. A compressible fluid at virtually zero velocity in the settling chamber is accelerated through the contraction section to sonic speed in the throat where, if the contraction section is properly designed, the flow is uniform and parallel. The fluid is then expanded in the nozzle until the desired Mach number is reached in the test section where the flow is again uniform and parallel. In the analysis, the nozzle itself is divided at the inflection point of the wall into two sections: initial and terminal.

6. It should be noted that there is one additional prerequisite for the establishment and perpetuation of supersonic flow. This is the maintenance of at least the minimum pressure ratio between the settling chamber (pressure = p_o) and the test section (pressure = p_t) from reference (e), page 26

$$\frac{p_o}{p_t} = \left(1 + \frac{\gamma-1}{2} M_t^2\right)^{\frac{\gamma}{\gamma-1}}, \qquad (1)$$

where M_t is the Mach number in the test section and γ is the ratio of the specific heats of the gas.

7. An isentropic supersonic flow through a two-dimensional nozzle may be treated by means of a few simple considerations. First, consider an incident unidimensional supersonic flow over a single curved surface. The change in local Mach number between any two points is a function only of the change in direction of the stream between the points or the change in direction of the tangents to the surface at these given points. To consider the flow field between two curved surfaces, however, it is convenient to replace each surface by an infinite number of infinitesimally long straight-line segments, or a finite number with discreet but small length. Each adjacent pair of lines thus constituted forms a corner. The supersonic flow about a corner is a classical problem and its solution is known. The flow between two curved surfaces thus reduces to the determination of the combined effect of two sets of corners. This introduces the problems of intersection and reflection of influence, or disturbance lines. In addition, the condition requiring uniform and parallel flow in the test section leads to the concept of neutralization of disturbance lines. The following sections will elucidate upon these concepts.

A. Flow About a Corner

8. The flow about a convex corner formed by two intersecting straight lines has been treated analytically by Prandtl and Meyer (reference f, pp. 243-246). For any such configuration, three regions of flow exist. These are indicated in Figure 2. The flow is uniform and parallel upstream and downstream of the corner in the regions I and III bounded by the surface and the corresponding disturbance or "Mach" lines. In the region II between these Mach lines, flow parameters are constant along radial lines (each of which is a Mach line) emanating from the vertex of the corner. The component of the velocity normal to a Mach line is equal to the local sound velocity, c.

9. The fundamental equation of flow-about-a-corner is (Figure 3)

$$\nu = \kappa \tan^{-1}\left(\frac{\cot\alpha}{\kappa}\right) - (90^\circ - \alpha) \quad , \tag{2}$$

where ν is the expansion angle or the angle through which the flow is turned in accelerating from a local Mach number of unity to any given Mach number M; α is the corresponding Mach angle

$$\alpha = \sin^{-1}\frac{1}{M}$$

and

$$\kappa^2 = \frac{\gamma+1}{\gamma-1} \quad .$$

Obviously, if ν is known in any region, the Mach number is determined by equation (2) and can be found.

10. The formula for the expansion angle, equation (2), can be derived in the following manner. The notation is defined on Figure 3. Since conditions are constant along radial lines, $\frac{\partial p}{\partial r} = 0$ and the only radial force is centrifugal. This force is then equal to the time-rate of change of momentum:

$$\frac{\rho v^2}{r} = \rho \frac{\partial u}{\partial t} = \rho \frac{\partial u}{\partial \varphi}\frac{\partial \varphi}{\partial t} \quad .$$

But the component of velocity normal to the Mach line, $v = r\frac{\partial \varphi}{\partial t} = c$, the local sonic speed. Thus we can write

$$\frac{\rho v^2}{r} = \frac{\rho v}{r}\frac{\partial u}{\partial \varphi}$$

or

$$v = \frac{\partial u}{\partial \varphi} = \frac{du}{d\varphi}$$

since u is not a function of r. Now the energy equation can be written

$$\frac{1}{2}V^2 + \frac{\gamma}{\gamma-1}\cdot\frac{p}{\rho} = \frac{1}{2}a^2 ,$$

where a is the ultimate velocity obtained by expanding the gas isentropically into a vacuum and $V^2 = u^2 + v^2$. Now $v^2 = c^2 = \gamma p/\rho$. Hence the energy equation takes the form $u^2 + \kappa^2 v^2 = a^2$. Substituting $v = \frac{du}{d\varphi}$ in this equation and solving for u we get $u = a \sin\frac{\varphi}{\kappa}$ and hence $v = \frac{a}{\kappa}\cos\frac{\varphi}{\kappa}$. But $\cot\alpha = \frac{u}{v} = \kappa \tan\frac{\varphi}{\kappa}$ and solving for φ we get $\varphi = \kappa \tan^{-1}\left(\frac{\cot\alpha}{\kappa}\right)$. Finally from the geometry of the figure,

$$\nu = \varphi - \left(\frac{\pi}{2} - \alpha\right)$$

and equation (2) follows immediately.

11. Referring now to Figure 2, let the subscripts 1 and 2 refer to conditions in the regions I and III, respectively. Then the angle through which the flow is turned in accelerating from a Mach number M_1 to M_2, that is, in going from region I to III, is

$$\delta = \nu_2 - \nu_1 \tag{3}$$

In other words, the change in expansion angle is equal to the absolute value of the change in stream deflection through an expansion region due to a single corner.

12. If the stream deflection angle δ is small, then all the expansion may be considered to take place along the average Mach line as shown in Figure 4. This line, no longer a line of propagation of an infinitesimal disturbance, now takes on certain characteristics of a shock wave; namely, the flow through it suffers a finite change in direction and Mach. It is usually referred to as an expansion wave. Little error is introduced by making these assumptions and, as δ approaches zero, the error vanishes. It is convenient to define the strength of a wave as the angular deflection of the stream that it produces,

B. Flow Parameters

13. Flow conditions are completely determined by the parameters ν, the expansion angle, and θ, the stream angle relative to some datum line usually taken as the flow direction in the throat. These coordinates are usually written

$$\nu, \theta \quad \text{or} \quad \begin{pmatrix}\nu \\ \theta\end{pmatrix}$$

C. Intersection of Expansion Waves

14. The problem of the interaction of the expansion waves from two opposed convex surfaces, such as the initial portion of a nozzle, may be considered in its elementary form: the intersection of two expansion waves as depicted in Figure 5.

15. It follows from reference (b), pp. 55-58, that the angular change in direction of the stream through an expansion wave is constant along its length regardless of the direction or velocity of the flow in front of the wave; that is to say that the expansion waves pass through each other mutually unaffected in strength, although their inclination is altered. Their effect on the flow may be determined by superposition of individual effects.

16. Consider the two expansion waves shown in Figure 5. For convenience, they are designated (1) and (2) and have strengths of $+\epsilon$ and $-\delta$, respectively. The upper streamline shown is deflected up through an angle ϵ by (1) and down through an angle δ by (2). The total angle through which it is deflected is thus $+\epsilon-\delta$. Similarly, the lower streamline is deflected first downward by (2) then upward by (1). Its final angle is the same as for the upper streamline and is equal to $\theta+\epsilon-\delta$. In a like manner, the final expansion angle can be found to be increased by $\epsilon+\delta$ for both streamlines.

D. Reflection of Expansion Waves by a Wall

17. Conditions resulting from the reflection of an expansion wave by a boundary may be determined by utilizing the well-known mirror-image concept. Thus, the wall may be replaced by a streamline in a fictitious flow comprised of the original flow, plus an image flow field, as shown in Figure 6. The problem of the reflection of expansion waves by a wall then becomes that of the intersection of expansion waves. The latter problem was the subject of the preceding section.

18. This concept may be applied in a converse manner in the design of symmetrical nozzles. In this case, the straight center line of the nozzle is replaced with a wall. Thus, the amount of work is halved.

E. Neutralization of Expansion Waves

19. If a shock wave of infinitesimal strength is superimposed on an expansion wave of equal strength (and by definition opposite in sign), the flow is unchanged after passing through both. This is also very nearly true if the waves have a finite but small strength. Therefore, if at the point where an expansion wave hits the wall a compression wave of equal strength is created, the expansion wave will be neutralized. Such a compression wave can be created, as illustrated in Figure 7, by an angular change in direction of the wall equal to the strength of the given expansion wave. The direction of the deflection should be such as to form a concave corner.

F. Flow in a Nozzle

20. The flow throughout a two-dimensional nozzle can be determined by use of the previously discussed concepts. The flow coordinates in the nozzles shown in Figures 8 and 9 are presented to illustrate the method. While symmetrical nozzles are discussed predominantly herein, the concepts involved apply to supersonic flows in general.

21. The angle between the wall at its inflection point and the center line (for symmetrical nozzles) is of importance in nozzle design. For shapes simulated by straight-line segments, this inflection point appears as a region. Let the subscript $_1$ refer to conditions in this region immediately preceding the point at which neutralization first takes place. These positions are denoted by arrows in Figures 8 and 9.

22. The following relation then becomes apparent from the numbers indicated in Figures 8 and 9:

$$\nu_1 + \theta_1 = \nu_t \quad . \tag{4}$$

In addition, since the angle θ_1 never can be greater than the expansion angle, ν_1, it is obvious that the maximum value that θ_1 can have for shock-free flow occurs when $\theta_1 = \nu_1$ or

$$\theta_{1_{max}} = \frac{1}{2}\nu_t \quad . \tag{5}$$

23. It should be noted that, if the initial curve is not approximated by straight-line segments, θ_1 can equal ν_1 only for a nozzle which has an abrupt expansion at the throat as shown in Figure 10. However, for such a nozzle, it is still possible for θ_1 to be less than $\frac{1}{2}\nu_t$ provided that some of the expansion waves are allowed to be reflected before they are neutralized.

24. For any smooth initial curve, that is, with no discontinuity in ordinate or slope from the sonic section to the inflection point, ν is greater than $|\theta|$ for $\theta \neq 0$. This condition appears to be violated in the nozzles shown in Figures 8 and 9, wherein there exist certain regions along the wall where ν equals θ. The explanation of this lies in the fact that the wall was simulated by a finite number of corners. The error introduced by this assumption is approximately given by

$$0 < \nu_{exact} - \nu_{approx} < \delta \quad ,$$

where δ is the angular deviation of each corner. In the cases illustrated in Figures 8 and 9, δ equals 2 degrees. Consequently, ν is actually greater than θ. This error is usually small and can be ignored without serious consequences.

25. For any given Mach number, while there are an infinite number of satisfactory nozzles, there is one invariant parameter: the ratio of the areas of the test section and throat (reference e, p. 34)

$$\frac{A_t}{A^*} = \frac{1}{M_t}\left[\frac{2+(\gamma-1)M_t^2}{\gamma+1}\right]^{\frac{1}{2}\cdot\frac{\gamma+1}{\gamma-1}} \tag{6}$$

where A is cross-section area (or height in a two-dimensional nozzle), the * refers to conditions in the throat (sonic section), and the subscript t refers to conditions in the test section.

III. Methods of Nozzle Design and Analysis

A. Busemann's Method

26. Busemann's method for designing nozzles (reference a) consists of assuming an initial curve and finding the terminal curve required to give uniform and parallel flow in the test section at the desired Mach number.

27. In order to design a nozzle for a Mach number M_t, first find the corresponding expansion angle ν_t . Assume an initial curve, and simulate it by a series of preferably equiangular corners. Then, starting at the throat and proceeding downstream, determine the flow field in terms of the parameters ν and θ . This is discussed from the theoretical point of view in preceding sections. In subsequent sections, actual methods of analysis will be described.

28. All expansion waves incident upon the wall upstream of the point where $\theta+\nu=\nu_t$ should be reflected and those incident downstream of this point should be neutralized. Thus, this point becomes the inflection point of the wall.

29. It is interesting to note that, while the initial curve is arbitrary, the corresponding terminal curve is unique once the initial curve is established.

30. For an infinitely fine mesh of expansion waves, this method is exact. Moreoever, for a finite mesh size, the finer it is, the more accurate is the analysis.

31. This method is, perhaps, the most useful in designing nonconventional nozzles, since for conventional types, the Foelsch method (to be described later) is more convenient.

B. Puckett's Method

32. Puckett, in reference (g), introduced a variation of Busemann's method for designing nozzles. Its advantages will be discussed subsequently. The method consists briefly of starting at the middle of the nozzle and working towards both ends.

33. The flow through the nozzle at the maximum expansion section (inflection point) is assumed to have a uniform speed and uniformly varying direction of flow. Such conditions are illustrated in Figure 11. The stipulation of these boundary conditions has been found from experience to be reasonable. With these boundary values, the terminal section of the nozzle can be determined by the same method as for the original type Busemann nozzles. By working backward in a like manner, an initial section can also be constructed, Moreover, if θ_1 is less than $\theta_{1\,max}$, then one or more of the expansion waves must have been reflected. Since there is a choice as to which wave is reflected, there is more than one initial curve that will provide the specified flow at the maximum expansion section. In fact, if the mesh size is allowed to become infinitely fine, then it follows that there are an infinite number of initial curves that correspond to this terminal curve. This same agreement obviously holds for initial curves corresponding to other terminal curves.

34. While, however, there are an infinite number of suitable initial curves for each terminal curve, this does not infer that any contour satisfying the area-ratio requirement is suitable. On the other hand, the error introduced by using an arbitrary curve can be ignored for most practical purposes, provided that a certain amount of care is taken. In a later section a simple method for the design of such initial sections will be discussed.

35. There are several advantages to Puckett's method. First, if the simplified method for designing the initial section is used, the time or work involved in designing a nozzle is approximately halved.

36. The second advantage becomes apparent during the actual calculation of nozzles. In the original Buseman method, expansion waves are originated at certain points along a smooth initial curve; that is, the spacing of the expansion waves is orderly, although it need not be uniform. When a finite mesh size is used, sometimes expansion waves are reflected from the wall at such points as to destroy the orderliness of the spacing of the ensuing expansion wave pattern. The resulting terminal curve thus acquires slight irregularities. These irregularities disappear as the mesh size becomes infinitely fine and, in practice, one usually draws a faired curve through them. The Puckett variation, however, avoids this difficulty.

C. Foelsch's Method

37. Foelsch's method (reference c) is similar to Puckett's insofar as one starts at the inflection point of the nozzle and proceeds in both directions. It differs slightly in boundary conditions but its main difference and direct advantage is that it is analytic. Only the portion of Foelsch's theory which deals with the expansion section will be discussed here.

38. The assumptions of this method, or rather its boundary conditions, may be variously stated (Figure 12): (1) Along the Mach line

emanating from the inflection point, the velocity vectors are cooriginal, (2) the Mach number is constant along the arc of the circle which passes through the inflection point of the wall perpendicularly (and obviously its center is the origin of the velocity vectors), (3) in the region between this arc and the Mach line from the inflection point, the Mach number is a function solely of the radius from the vector origin.

39. Using the following notation (Figure 12)

r distance from vector origin to arbitrary point on inflection point Mach line

r_o hypothetical r for M = 1

l length of Mach line between inflection-point Mach line and terminal curve

x coordinate measured from sonic section

y coordinate measured from center line

x_1, y_1 coordinates of inflection point

x_2, y_2 running coordinates of inflection-point Mach line

y_o semiheight of sonic section of nozzle

H height of test section ($2y_t$)

it can be shown that

$$r_o = \frac{y_o}{\theta_1} \qquad (\theta_1 \text{ in radians}) \tag{7}$$

$$r = r_o \cdot \frac{A}{A^*} \tag{8}$$

$$r_1 = r_o \cdot \frac{A_1}{A^*} = \frac{y_1}{\sin\theta_1} \tag{9a}$$

or

$$\frac{y_1}{y_o} = \frac{\sin\theta_1}{\theta_1} \cdot \frac{A_1}{A^*} \qquad \theta_1 \text{ in radians} \tag{9b}$$

$$l = Mr(\nu - \nu_1) \qquad \nu \text{ in radians} \tag{10}$$

$$x_2 - x_1 = -r_1 \cos\theta_1 + r\cos(\nu_1 - \nu) \tag{11a}$$

$$y_2 = r\sin(\nu_t - \nu) \tag{11b}$$

and the coordinates of the terminal curve are

$$x - x_1 = x_2 - x_1 + l\cos(\nu_t - \nu + \alpha) \tag{12a}$$

$$y = y_2 + l\sin(\nu_t - \nu + \alpha) \tag{12b}$$

and length of the terminal section (in test-section heights) is

$$\frac{x_t - x_1}{H} = \frac{\sqrt{M_t^2 - 1}}{2} + \frac{1}{2\theta_1}\left(1 - \frac{A^*}{A_t}\cdot\frac{A_1}{A^*}\cos\theta_1\right) \quad (\theta_1 \text{ in radians}) \tag{13}$$

40. By varying the Mach number M along the terminal curve from M_1 to M_t and determining the corresponding values of α, ν, r and l, the coordinates of the terminal curve can be found and are determined as a function of conditions in the test section and at the inflection point. Table I is included to facilitate these calculations. The initial curve, as for the Puckett method, may be treated separately.

41. It can be seen that the methods of Puckett and Foelsch are quite similar with regard to boundary conditions, the former having a constant Mach number along a straight line and the latter along a circular arc. Both assumptions are equally plausible. The difference between these assumptions manifests itself in a slight and inconsequential lengthening of the Foelsch nozzle relative to the corresponding Puckett nozzle.

42. The analytic nature of the Foelsch method allows nozzles to be determined to any desired degree of accuracy and without any such apparatus (to be described later) as that required for the graphical methods.

43. It is interesting to observe that this method is one of the few exact analytic solutions of the general nonlinear potential equation for two-dimensional compressible supersonic flow.

D. <u>The Initial Curve</u>

44. The initial curve, either exact or approximate, must satisfy certain geometric boundary conditions: It must satisfy the area-ratio requirements. It must have zero slope at the sonic section and the same ordinate, slope, and curvature (zero) at the inflection point as the terminal curve. The ordinate, slope, and curvature should vary monotonically between the sonic section and the inflection point. A simple

function satisfying these limitations is

$$y = y_0 + \left(\frac{\tan\theta_1}{x_1}\right) x^2 \left(1 - \frac{x}{3x_1}\right) \tag{14}$$

from which it follows that

$$x_1 = \frac{3}{2}(y_1 - y_0)\cot\theta_1 \quad , \tag{15}$$

where y_1 follows from eq. (9b).

45. Experience has shown that this approximate initial-curve function can be used for both the Puckett and Foelsch methods without any serious error. For the original-type Busemann method, this curve can be simulated by appropriate straight-line segements.

E. Analysis of Nozzles

46. The analysis of given nozzles to determine the velocity distribution in the test section and to ascertain the existence or non-existence of shock waves is a process very similar to the design of nozzles. In fact, the procedure for the initial portion of the nozzle is identical.

47. In the terminal section, instead of neutralizing the expansion waves, they are all reflected and compression waves started at appropriate places. For small angular deflections, compression waves may be considered simply as negative expansion waves. In practice, where an expansion wave is incident upon a wall near the position where a compression wave (of the same numerical strength, but opposite sign) originates, they may be considered to neutralize each other.

48. Thus from the coordinates ν and θ, the velocity distribution in the test section can be found. The location of possible shock waves is indicated by a region of converging Mach lines (or compression waves) - the greater the concentration of converging waves, the stronger the shock. A weak concentration of slowly converging waves may be too weak to show up in a schlieren photograph or to have any noticeable effect; hence, the term "possible" shock waves are used. A nozzle exhibiting a region of converging waves is shown schematically in Figure 14.

IV. Effect of Variation of Parameters

49. The major parameter involved in the design of nozzles is θ_1 or, perhaps, rather $\theta_1/\frac{1}{2}\nu_t$. The length of the nozzle is intimately associated with this parameter.

50. As previously stated, the maximum value that θ_1 can have for shock-free flow at a given Mach number is $\frac{1}{2}\nu_t$. A nozzle so designed will be the shortest possible for that Mach number and must

have a sharp throat such as the one shown in Figure 10 with $\nu_1 = \frac{1}{2}\nu_t$ The other extreme in designing nozzles is setting $\theta_1 = 0$. This would quire that the nozzle have infinite length.

51. There are, of course, certain obvious disadvantages in designing a nozzle too long or too short. An excessively long nozzle incurs adverse boundary-layer effects of two kinds: First, the longer the nozzle, the thicker the boundary layer, other conditions being the same. Since boundary-layer thickness is, at the present time, not very amenable to precise calculation, a given percent error in boundary-layer calculation is more serious when the boundary layer is thick. The result is that flow in the test section is less likely to be uniform, parallel, and shock free. Second, a thicker boundary layer represents an unnecessary waste of energy.

52. An excessively short nozzle, on the other hand, is liable to other troubles. A minimum-length nozzle has for a given Mach number, the maximum number of expansion waves (considering each to be of finite strength) concentrated into the minimum space. A longer nozzle achieves the same Mach number by reflecting some of the waves. Thus, it has fewer of them and these are extended over a wider range. This is to say that the expansion waves are more concentrated in shorter nozzles. It is then apparent that they are more sensitive to proper design than longer ones. Designing nozzles to be somewhat longer than the minimum incorporates what might be termed a safety factor. In addition, there is less likelihood for such a nozzle to have oscillatory flow.

53. The tendency at some German laboratories was to design nozzles with lengths equal to or slightly greater than the minimum. While most of these nozzles were claimed to be satisfactory, subsequent experience has shown that small gradients previously believed negligible have been found to exert strong influences on test results.

54. Puckett, in reference (g), suggests using θ_1 equal to from one half to two thirds of $\theta_{1\,max}$ $\left(= \frac{1}{2}\nu_t\right)$. It is believed that at low Mach numbers such nozzles will be unnecessarily long.

55. At the present time there are insufficient experimental data to say exactly how a nozzle should be designed. However, experience up to the present time indicates that a value of

$$\theta_1 \simeq \left(\frac{A^*}{A_t}\right)^{\frac{2}{9}} \frac{\nu_t}{2} \qquad \text{(for air)} \qquad (16)$$

will provide a good working hypothesis.

56. The preceding equation is restricted to air only because of the limitations of past experience. The general considerations discussed herein, however, apply to helium or any other compressible fluid.

V. Construction of Flow Field - Supersonic Protractor

57. The determination of the flow field in a nozzle has been discussed previously from the theoretical point of view. It remains now to show how to construct or determine the orientation of each of the Mach line (or expansion wave) segments which make up the net that determines the flow field. (See Figures 8 and 9.)

58. Various methods have been proposed to do this. Analytic methods, such as the one described in reference (h), have been devised but are extremely tedious. Graphical methods have been found sufficiently accurate for most design or analysis purposes. On the other hand, the analytic nature of the Foelsch method allows ordinates to be determined simply and precisely. The main use of the Busemann theory is, at the present time, usually restricted to the design of nonconventional nozzle shapes and the analysis of any given shape.

59. A graphical method based on the use of characteristic theory and the hodograph plane is described in reference (b). However, this method has been superseded by the so-called "supersonic protractor" (reference i), a modification of which is described herein.

61. It is assumed that conditions along an expansion wave are the average of those in the regions it separates. Each segment is thus characterized by the pair of coordinates ν and θ. For each value of ν and θ, there are two possible orientations of an expansion wave. These correspond to the two Mach lines produced by a point disturbance. The angle made by an expansion wave with the datum line is $\theta + \alpha$ for the wave directed upward in the stream direction and $\theta - \alpha$ for the one directed similarly downward. These two cases are shown in Figure 14.

62. The supersonic protractor has two essential parts which may be described independently. The first, shown in Figures 15(a) and 15(b), consists of a semi-circular transparent disk, pivoted at its center, and with a straight edge attached. It is graduated along its circumference such that when the desired ν is set over the datum line, for example, $\nu = 30^\circ$, α is represented as shown. That this is possible follows from equation (2):

$$\nu = \kappa \tan\left(\frac{\cot \alpha}{\kappa}\right) - (90^\circ - \alpha). \qquad (2)$$

63. The second piece, shown in Figure 16, consists simply of a circular disk graduated along its circumference in degrees. This scale represents the stream direction θ.

64. If the former part of the protractor, that providing α, is rotated through an angle equal to the stream direction θ, the required orientation of the Mach line (or expansion wave) is thus determined. This is accomplished with the protractor by superimposing the former upon the latter concentrically and rotating the former until the desired ν

is set over the desired θ . This is shown schematically in Figures 17(a) and 17(b), and the similarity of these with Figure 13 should be noted. Thus, while the end points of certain expansion-wave segments may be dependent upon the previous one, each in its turn can be orientated simply by means of this protractor, knowing, of course, ν and Θ .

65. Table II, containing values of α corresponding to even values of ν , is included for calibrating the supersonic protractor. It should be noted that if the amount of work involved does not justify the construction of this protractor, a drafting machine may be substituted. In this case, $\theta \pm \alpha$ can be set with the aid of Table II.

VI. Boundary Layer

66. Air is not an inviscid fluid and thus does not satisfy the assumptions on which the fundamental equations of the designing methods are based. A boundary layer will develop along the nozzle walls which is not allowed for in the theoretical treatment. Between the "boundary-layer walls," however, the flow will behave as an ideal gas (Figure 18). It seems self-evident that in order to get the appropriate nozzle contour one has simply to add a "boundary-layer thickness-correction" to the ordinates obtained as described in the foregoing sections. Unfortunately there exists no formula from which to compute this thickness in the case of supersonic accelerated motion past curved surfaces. Reference (j) contains a method for estimating boundary-layer thickness. A small amount of experimental boundary-layer data is included in reference (g). Eaton and Deacon, reference (k), used such estimated values for a nozzle they designed, but state that the actual thickness proved to be considerably greater.

67. It was learned from nozzles built and tested in Germany and elsewhere that the influence of the boundary layer becomes noticeable only towards the end of the test section, where the Mach number was found to be decreasing. This indicates that the air was prevented from expanding sufficiently in the last portion of the nozzle, owing to the too small cross sections between the boundary-layer walls. The inference was drawn that the nozzle's mouth must be opened slightly more than the frictionless theory would require. In fact, the boundary-layer walls at the end of the nozzle are not parallel, and thus the flow cannot be expected to be uniform. They can be made parallel, however, if the physical walls are allowed to diverge by a small angle.

68. The boundary layer is visible in schlieren pictures. Though one may doubt whether the actual boundary-layer thickness is depicted, one may assume that the slope toward the nozzle's mouth will not deviate much from the slope of the actual boundary-layer wall. If η_E is the angle that the tangent to the boundary layer drawn in W_E (Figure 19) makes with the axis, then $\tan \eta_E$ was found in the range between 0.004 and 0.010. This is consistent with values given by Puckett (reference g) according to measurements made in the 2.5-in. wind tunnel at the GALCIT (0.007 to 0.010).

69. After designing the nozzle, one is able to plot the values $\tan\eta$ against the abscissa x (Figure 19), beginning at the point of maximum wall slope (C). The curve thus obtained is qualitatively indicated in Figure 20; it represents the slope of the physical wall, which is zero at the nozzle's end. If the nozzle is opened by a suitable angle η_E, the boundary-layer walls will become parallel in the exit area. Thus the original curve has to be modified tentatively in the manner shown in Figure 20. The ordinates downstream from the point M_C at which the deviation from the original curve begins will be found from:

$$y = y_{M_C} + \int_{x}^{x_{M_C}} \tan\eta \, dx \tag{17}$$

where the modified values of $\tan\eta$ are used. The integral, as a rule, must be evaluated numerically.

VII. Nozzle Correction

70. A nozzle made according to one of the procedures outlined in the foregoing sections may sometimes prove to be satisfactory, but in many cases will not produce a sufficiently uniform flow in the test section. Several causes which may prevent uniform flow may be listed:

(1) The approximate methods render a polygonally shaped wall instead of a continuous curve. The initial curve defined by (14), though continuous, is not derived from an exact solution of the underlying differential equation.
(2) The manufacture cannot be exact.
(3) The sonic line is, in fact, not a straight line though it is taken as such by Busemann's method. If the Puckett or Foelsch methods are employed, the velocity distribution over the maximum expansion section may have been incorrectly assumed.
(4) The boundary-layer influence may not have been properly estimated.

71. It is, therefore, desirable to possess a means for correcting a nozzle. We shall at first substitute for air an ideal gas that lends itself to a treatment according to the Prandtl-Busemann rules. Subsequently certain modifications due to the boundary layer will be incorporated, if this still appears necessary.

72. The flow state in the test section can be investigated in various ways. Measurements of static pressure, pitot pressure, shock angles, and Mach angles may be performed. The purpose of nozzle correction is served best by the Mach-angle survey. Conditions along the walls give rise to disturbance wavelets propagating some slight density jump which, by the powerful means of a sensitive schlieren apparatus, can be made visible and photographed. Thus the test section appears traversed by lines which originate on both walls and make the local Mach

angle with the nozzle axis. One of those Mach lines belonging to the upper family, is shown on Figure 19. If a sufficiently large number of disturbance lines is utilized a fairly complete picture of the Mach-angle distribution along the test-section axis will be obtained. If any irregularities exist, they will be detected and can be traced to their origin on either wall. The latter feature accounts for the superiority of the wavelet method. None of the other measurements, though the Mach angles can be computed from their results, will permit locating with equal exactness the origin of the irregularity for the following reason. The test section, in which the flow is already nearly uniform, is bounded, upstream, by two Mach lines running through the points E and E' (Figure 21). Outside these Mach lines the disturbance wavelets will no longer remain rectilinear (as they have been inside the test section), because they pass a region of changing flow state and, therefore, of changing Mach angle and flow direction. Thus it is difficult to trace a wavelet back to its origin, unless it is visible. The Mach angle at A can be derived from pressure measurement, but it will not determine the location of W.

73. To know the wavelet origin, however, is decisive as regards the nozzle correction. For the wall is, in terms of mathematics, the boundary condition which accounts largely for developing the flow pattern. Every irregularity of the contour will be propagated along a disturbance line into the stream and will, at the spot where the line cuts the axis, be noticeable as an irregularity in flow state, e.g., in Mach-angle distribution. This faulty state, then, cannot be done away with except by appropriately altering the boundary at the point at which it originated. If a uniform flow is reached along the test-section axis there is little likelihood of encountering major deviation in flow uniformity anywhere else in the test section. It appears highly improbable that wall irregularities should interact so that the axis flow alone would be uniform. The correction method to be advanced subsequently aims at correcting the flow state along the axis only. This is recommended also by the fact that the test models, as a rule, are placed near the axis.

74. The conclusion to be drawn from the previous statements is that the relationship between the abscissae, z, of the points A_i lying on the test section axis, and the abscissae, x, of the corresponding wall points W_i must first be established (cf., Figure 19).

75. The disturbance wavelets appearing on a schlieren picture of the interesting part of the nozzle follow the Mach lines connecting the points A_i with the points W_i. Evaluating such a picture one is able to plot x against z; if a curve is faired through the discrete measurement points, a continuous correlation between z and x will be obtained (Figure 22). Negative values of z occur, because the test section extends downstream from the nozzle mouth (z = 0) until the axis point $\bar{A}$ (Figure 21) is reached, where the two Mach lines originating at E and E' (x = 0) intersect. Obviously, there is no point in investigating the axis flow beyond $\bar{A}$ because it is no longer influenced by the nozzle wall and thus cannot be corrected.

76. The boundary condition is the slope of the wall, which determines the direction of the flow past the wall. The slope, therefore, has to be corrected if the desired uniform state within the test section has not been achieved.

Figure 23 illustrates what will happen if the wall, at two opposite points, is bent by $\Delta\eta$. Both bends can be regarded as elementary Prandtl-Meyer-corners. Accordingly, two Mach lines will arise at W_i and W_i' along which the expansion angle changes everywhere by $\Delta\theta = \Delta\eta$. Since these lines are either both expansion waves or both compression waves, the effect at the axis point A_i (where they meet) will be doubled, so that the original expansion angle at A_i is altered by $2\Delta\eta$. Conversely, if one wishes to change the expansion angle at A_i by $\Delta\theta$ the wall slope at W_i and W_i' must be altered by $\Delta\eta = 1/2\,\Delta\theta$.

77. Suppose now that evaluation of schlieren pictures has shown a distribution of Mach angles along the axis as sketched on Figure 24. In order to smooth this curve by nozzle correction we shall at first select a suitable median Mach angle, μ^*, which is to result from the correction. This angle must not be taken too large. For, enlarging the Mach angle means diminishing the wall slope, and this may give rise to the work-shop predicament that the wall must be thickened.

78. If, at any point A_i, the Mach angle μ_i deviates from μ^* we shall use the expansion angles θ_i and θ^* that correspond to μ_i and μ^*, to determine that correction:

$$\Delta\eta_i = 1/2\,(\theta^* - \theta_i).$$

At the wall point W_i, then, the original inclination η_i has to be changed to:

$$\bar{\eta}_i = \eta_i + \Delta\eta_i .$$

The values η_i should not be taken from the nozzle design. Instead, those values should be used as have arisen in actually making the nozzle.

79. From Figure 22 we can find the abscissae x_i of the wall points W_i and are now able to plot $\tan\eta_i$ and $\tan\bar{\eta}_i$ against x_i (Figure 25). The distribution assumed in Figure 24 shows, in the (-z) direction, a steady increase of the Mach angle near the downstream limit of the test section. This indicates that the boundary-layer influence has not properly been dealt with in designing the nozzle. The continually increasing deviation from μ^* will result in a similar behavior of $\tan\bar{\eta}_i$ compared to $\tan\eta_i$ near the nozzle's end (see Figure 25). These values of $\tan\bar{\eta}_i$ as affected by the boundary layer, should not be given much weight, in view of the fact that the correction procedure is based on the assumption of a nonviscous fluid. Using schlieren pictures a careful investigation should be made of the inclination, η_E, of the "boundary-layer wall" at the exit. The curve $\tan\bar{\eta} = f(x)$ which is to be faired through the discrete correction points of Figure 25 must be drawn to cross the vertical axis at the ordinate $\tan\eta_E$ or in the

immediate vincinity, without much concern as to the position of the last uncertain correction points.

80. If x_c, y_c are the coordinates of the wall points C, the corrected ordinates will be found from a relation analogous to (17):

$$y = y_c + \int_{x}^{x_c} \tan \bar{\eta} \, dx. \tag{18}$$

Upon evaluation of this integral for an appropriate number of abscissae x, the correction is finished.

VIII. Concluding Remarks

81. Using the methods discussed in this report, it is possible to design satisfactory nozzles either graphically or analytically. While the analytic method is to be preferred in design, the graphic method can be extended to include the analysis of given nozzle shapes to determine flow characteristics. A supersonic protractor which permits rapid graphical analysis and design is described. A correction method for nozzle contours has also been described.

J. Conrad Crown

J. Conrad Crown

Willi H. Heybey

Willi H. Heybey

JCC:WHH:hhh

TABLE I*- ESSENTIAL PARAMETERS USED IN NOZZLE DESIGN
$\gamma = 1.400$ (air)

M	$\frac{P}{P_o}$	$\frac{A^*}{A}$	α (deg)	ν (deg)	M	$\frac{P}{P_o}$	$\frac{A^*}{A}$	α (deg)	ν (deg)
1.00	0.5283	1.0000	90.00	0	1.50	0.2724	0.8502	41.81	11.91
1.01	.5221	.9999	81.93	.04473	1.52	.2646	.8404	41.14	12.49
1.02	.5160	.9997	78.64	.1257	1.54	.2570	.8304	40.49	13.09
1.03	.5099	.9993	76.14	.2294	1.56	.2496	.8203	39.87	13.68
1.04	.5039	.9987	74.06	.3510	1.58	.2423	.8101	39.27	14.27
1.05	.4979	.9980	72.25	.4874	1.60	.2353	.7998	38.68	14.86
1.06	.4919	.9971	70.63	.6367	1.62	.2284	.7895	38.12	15.45
1.07	.4860	.9961	69.16	.7973	1.64	.2217	.7791	37.57	16.04
1.08	.4800	.9949	67.81	.9680	1.66	.2151	.7686	37.04	16.63
1.09	.4742	.9936	66.55	1.148	1.68	.2088	.7581	36.53	17.22
1.10	.4684	.9921	65.38	1.336	1.70	.2026	.7476	36.03	17.81
1.11	.4626	.9905	64.28	1.532	1.72	.1966	.7371	35.55	18.40
1.12	.4568	.9888	63.23	1.735	1.74	.1907	.7265	35.08	18.98
1.13	.4511	.9870	62.25	1.944	1.76	.1850	.7160	34.62	19.56
1.14	.4455	.9850	61.31	2.160	1.78	.1794	.7054	34.18	20.15
1.15	.4398	.9828	60.41	2.381	1.80	.1740	.6949	33.75	20.73
1.16	.4343	.9806	59.55	2.607	1.82	.1688	.6845	33.33	21.30
1.17	.4287	.9782	58.73	2.839	1.84	.1637	.6740	32.92	21.88
1.18	.4232	.9758	57.94	3.074	1.86	.1587	.6636	32.52	22.45
1.19	.4178	.9732	57.18	3.314	1.88	.1539	.6533	32.13	23.02
1.20	.4124	.9705	56.44	3.558	1.90	.1492	.6430	31.76	23.59
1.21	.4070	.9676	55.74	3.806	1.92	.1447	.6328	31.39	24.15
1.22	.4017	.9647	55.05	4.057	1.94	.1403	.6226	31.03	24.71
1.23	.3964	.9617	54.39	4.312	1.96	.1360	.6125	30.68	25.27
1.24	.3912	.9586	53.75	4.569	1.98	.1318	.6025	30.33	25.83
1.25	.3861	.9553	53.13	4.830	2.00	.1278	.5926	30.00	26.38
1.26	.3809	.9520	52.53	5.093	2.02	.1239	.5828	29.67	26.93
1.27	.3759	.9486	51.94	5.359	2.04	.1201	.5730	29.35	27.48
1.28	.3708	.9451	51.38	5.627	2.06	.1164	.5634	29.04	28.02
1.29	.3658	.9415	50.82	5.898	2.08	.1128	.5538	28.74	28.56
1.30	.3609	.9378	50.28	6.170	2.10	.1094	.5444	28.44	29.10
1.31	.3560	.9341	49.76	6.445	2.12	.1060	.5350	28.14	29.63
1.32	.3512	.9302	49.25	6.721	2.14	.1027	.5258	27.86	30.16
1.33	.3464	.9263	48.75	7.000	2.16	.09956	.5167	27.58	30.69
1.34	.3417	.9223	48.27	7.279	2.18	.09650	.5077	27.30	31.21
1.35	.3370	.9182	47.79	7.561	2.20	.09352	.4988	27.04	31.73
1.36	.3323	.9141	47.33	7.844	2.22	.09064	.4900	26.77	32.25
1.37	.3277	.9099	46.88	8.128	2.24	.08785	.4813	26.51	32.76
1.38	.3232	.9056	46.44	8.413	2.26	.08514	.4727	26.26	33.27
1.39	.3187	.9013	46.01	8.699	2.28	.08252	.4643	26.01	33.78
1.40	.3142	.8969	45.58	8.987	2.30	.07997	.4560	25.77	34.28
1.42	.3055	.8880	44.77	9.565	2.32	.07751	.4478	25.53	34.78
1.44	.2969	.8788	43.98	10.15	2.34	.07512	.4397	25.30	35.28
1.46	.2886	.8695	43.23	10.73	2.36	.07281	.4317	25.07	35.77
1.48	.2804	.8599	42.51	11.32	2.38	.07057	.4239	24.85	36.26

*This Table appeared in NACA TN 1651 by J. C. Crown, dated June 1948.

TABLE I - CONTINUED. ESSENTIAL PARAMETERS USED IN NOZZLE DESIGN

M	$\frac{P}{P_o}$	$\frac{A^*}{A}$	α (deg)	ν (deg)	M	$\frac{P}{P_o} \times 10^3$	$\frac{A^*}{A}$	α (deg)	ν (deg)
2.40	0.06840	0.4161	24.62	36.75	4.00	6.586	0.09329	14.48	65.78
2.42	.06630	.4085	24.41	37.23	4.10	5.769	.08536	14.12	67.08
2.44	.06426	.4010	24.19	37.71	4.20	5.062	.07818	13.77	68.33
2.46	.06229	.3937	23.99	38.18	4.30	4.449	.07166	13.45	69.54
2.48	.06038	.3864	23.78	38.66	4.40	3.918	.06575	13.14	70.71
2.50	.05853	.3793	23.58	39.12	4.50	3.455	.06038	12.84	71.83
2.52	.05674	.3722	23.38	39.59	4.60	3.053	.05550	12.56	72.92
2.54	.05500	.3653	23.18	40.05	4.70	2.701	.05107	12.28	73.97
2.56	.05332	.3585	22.99	40.51	4.80	2.394	.04703	12.02	74.99
2.58	.05169	.3519	22.81	40.96	4.90	2.126	.04335	11.78	75.97
2.60	.05012	.3453	22.62	41.41	5.00	1.890	.04000	11.54	76.92
2.62	.04859	.3389	22.44	41.86	5.1	1.683	.03694	11.31	77.84
2.64	.04711	.3325	22.26	42.31	5.2	1.501	.03415	11.09	78.73
2.66	.04568	.3263	22.08	42.75	5.3	1.341	.03160	10.88	79.60
2.68	.04429	.3202	21.91	43.19	5.4	1.200	.02926	10.67	80.43
2.70	.04295	.3142	21.74	43.62	5.5	1.075	.02712	10.48	81.24
2.72	.04165	.3083	21.57	44.05	5.6	.9643	.02516	10.29	82.03
2.74	.04039	.3025	21.41	44.48	5.7	.8664	.02337	10.10	82.80
2.76	.03917	.2968	21.24	44.91	5.8	.7794	.02172	9.928	83.54
2.78	.03799	.2912	21.08	45.33	5.9	.7021	.02020	9.758	84.26
2.80	.03685	.2857	20.92	45.75	6.0	.6334	.01880	9.594	84.96
2.82	.03574	.2803	20.77	46.16	6.1	.5721	.01752	9.435	85.63
2.84	.03467	.2750	20.62	46.57	6.2	.5174	.01634	9.282	86.29
2.86	.03363	.2698	20.47	46.98	6.3	.4684	.01525	9.133	86.94
2.88	.03263	.2648	20.32	47.39	6.4	.4247	.01424	8.989	87.56
2.90	.03165	.2598	20.17	47.79	6.5	.3855	.01331	8.850	88.17
2.92	.03071	.2549	20.03	48.19	6.6	.3503	.01245	8.715	88.76
2.94	.02980	.2500	19.89	48.59	6.7	.3187	.01165	8.584	89.33
2.96	.02891	.2453	19.75	48.98	6.8	.2902	.01092	8.457	89.89
2.98	.02805	.2407	19.61	49.37	6.9	.2646	.01024	8.333	90.44
3.00	.02722	.2362	19.47	49.76	7.0	.2416	.009602	8.213	90.97
3.05	.02526	.2252	19.14	50.71	7.1	.2207	.009015	8.097	91.49
3.10	.02345	.2147	18.82	51.65	7.2	.2019	.008469	7.984	92.00
3.15	.02177	.2048	18.51	52.57	7.3	.1848	.007961	7.873	92.49
3.20	.02023	.1953	18.21	53.47	7.4	.1694	.007490	7.766	92.97
3.25	.01880	.1863	17.92	54.35	7.5	.1554	.007050	7.662	93.44
3.30	.01748	.1777	17.64	55.22	7.6	.1427	.006641	7.561	93.90
3.35	.01625	.1695	17.37	56.07	7.7	.1312	.006259	7.462	94.34
3.40	.01513	.1617	17.10	56.91	7.8	.1207	.005903	7.366	94.76
3.45	.01408	.1543	16.85	57.73	7.9	.1111	.005571	7.272	95.21
3.50	.01311	.1473	16.60	58.53	8.0	.1024	.005260	7.181	95.62
3.60	.01138	.1342	16.13	60.09	8.1	.09448	.004970	7.092	96.03
3.70	.009903	.1224	15.68	61.60	8.2	.08723	.004698	7.005	96.43
3.80	.008629	.1117	15.26	63.04	8.3	.08060	.004444	6.920	96.82
3.90	.007532	.1021	14.86	64.44	8.4	.07454	.004206	6.837	97.20

TABLE I - CONCLUDED

ESSENTIAL PARAMETERS USED IN NOZZLE DESIGN

M	$\frac{P}{P_o} x10^3$	$\frac{A^*}{A} x10^3$	α (deg)	ν (deg)
8.5	0.06896	3.981	6.756	97.68
8.6	.06390	3.773	6.677	97.94
8.7	.05923	3.577	6.600	98.29
8.8	.05494	3.392	6.525	98.64
8.9	.05101	3.219	6.451	98.98
9.0	.04739	3.056	6.379	99.32
9.1	.04405	2.903	6.309	99.65
9.2	.04099	2.759	6.240	99.97
9.3	.03816	2.623	6.173	100.28
9.4	.03555	2.495	6.107	100.59
9.5	.03314	2.374	6.042	100.89
9.6	.03092	2.261	5.979	101.19
9.7	.02886	2.153	5.917	101.48
9.8	.02696	2.052	5.857	101.76
9.9	.02520	1.956	5.797	102.04
10.0	.02356	1.866	5.739	102.32

TABLE II*- PARAMETERS USED IN CALIBRATING SUPERSONIC PROTRACTOR
γ = 1.400 (air)

ν (deg)	M	α (deg)	ν (deg)	M	α (deg)
0	1.0000	90.00	44	2.7179	21.59
1	1.0808	67.70	45	2.7643	21.21
2	1.1328	61.96	46	2.8120	20.83
3	1.1770	58.17	47	2.8610	20.46
4	1.2170	55.29	48	2.9105	20.09
5	1.2554	52.77	49	2.9616	19.73
6	1.2935	50.63	50	3.0131	19.38
7	1.3300	48.75	51	3.0660	19.06
8	1.3649	47.11	52	3.1193	18.70
9	1.4005	45.57	53	3.1737	18.38
10	1.4350	44.18	54	3.2293	18.04
11	1.4688	42.92	55	3.2865	17.72
12	1.5028	41.72	56	3.3451	17.40
13	1.5365	40.60	57	3.4055	17.08
14	1.5710	39.53	58	3.4675	16.76
15	1.6045	38.54	59	3.5295	16.46
16	1.6380	37.63	60	3.5937	16.16
17	1.6723	36.73	62	3.7288	15.56
18	1.7061	35.88	64	3.8690	14.98
19	1.7401	35.08	66	4.0164	14.42
20	1.7743	34.31	68	4.1738	13.86
21	1.8090	33.54	70	4.3385	13.33
22	1.8445	32.83	72	4.5158	12.79
23	1.8795	32.15	74	4.7031	12.28
24	1.9150	31.49	76	4.9032	11.76
25	1.9502	30.85	78	5.119	11.27
26	1.9861	30.23	80	5.349	10.78
27	2.0222	29.64	82	5.595	10.29
28	2.0585	29.06	84	5.867	9.81
29	2.0957	28.49	86	6.155	9.35
30	2.1336	27.97	88	6.472	8.88
31	2.1723	27.41	90	6.820	8.43
32	2.2105	26.90	92	7.202	7.98
33	2.2492	26.40	94	7.623	7.54
34	2.2885	25.91	96	8.093	7.10
35	2.3288	25.43	98	8.622	6.67
36	2.3688	24.99	100	9.210	6.23
37	2.4108	24.53	102	9.887	5.80
38	2.4525	24.07	104	10.658	5.38
39	2.4942	23.64	108	12.58	4.56
40	2.5372	23.22	112	15.37	3.73
41	2.5810	22.80	116	19.70	2.91
42	2.6254	22.38	120	27.29	2.10
43	2.6716	21.98	124	44.08	1.30

*This Table appeared in NACA TN 1651 by J. C. Crown, dated June 1948.

Unclassified

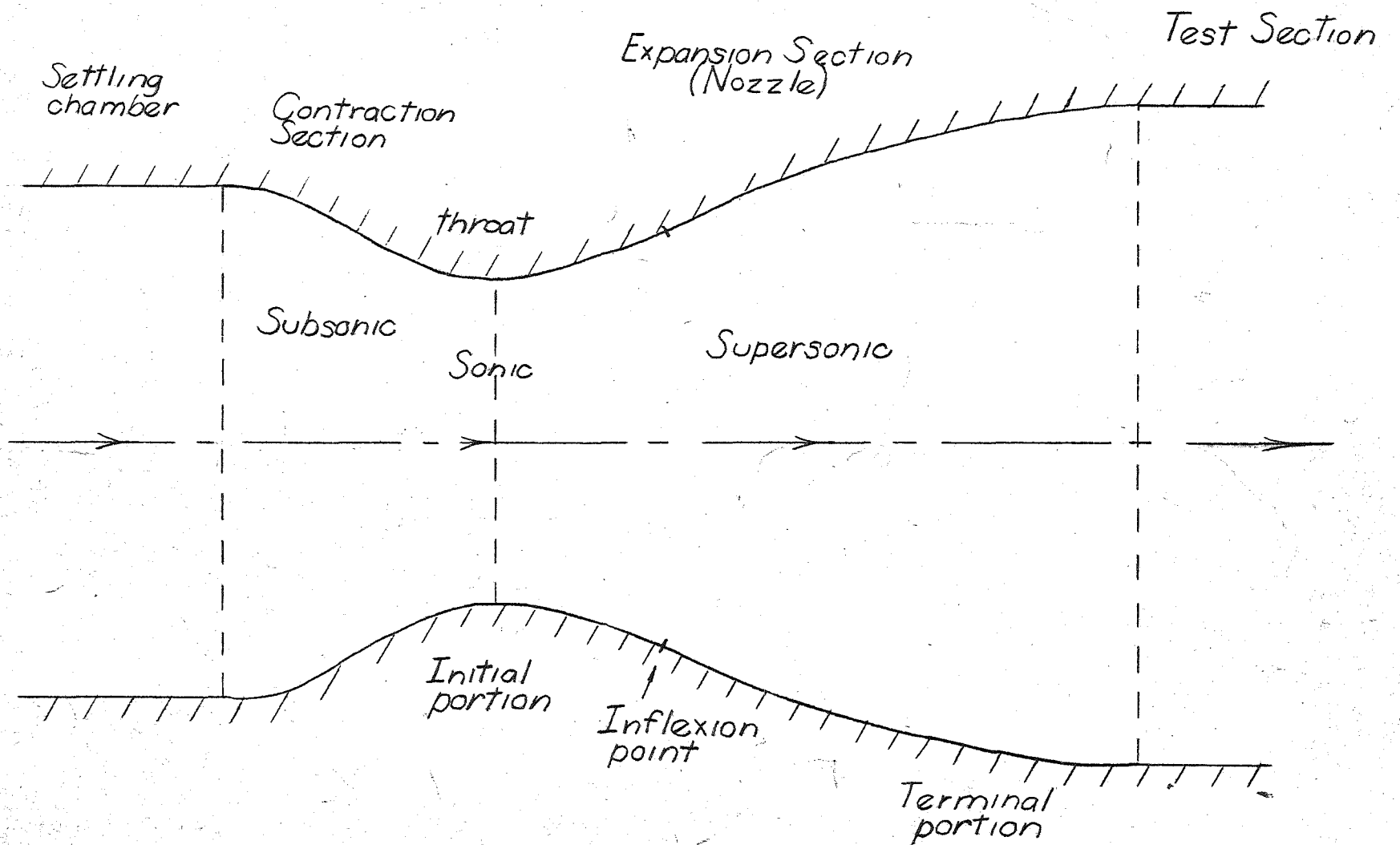

Fig. 1 Section of supersonic wind tunnel showing relative position of nozzle

NOLM 10594

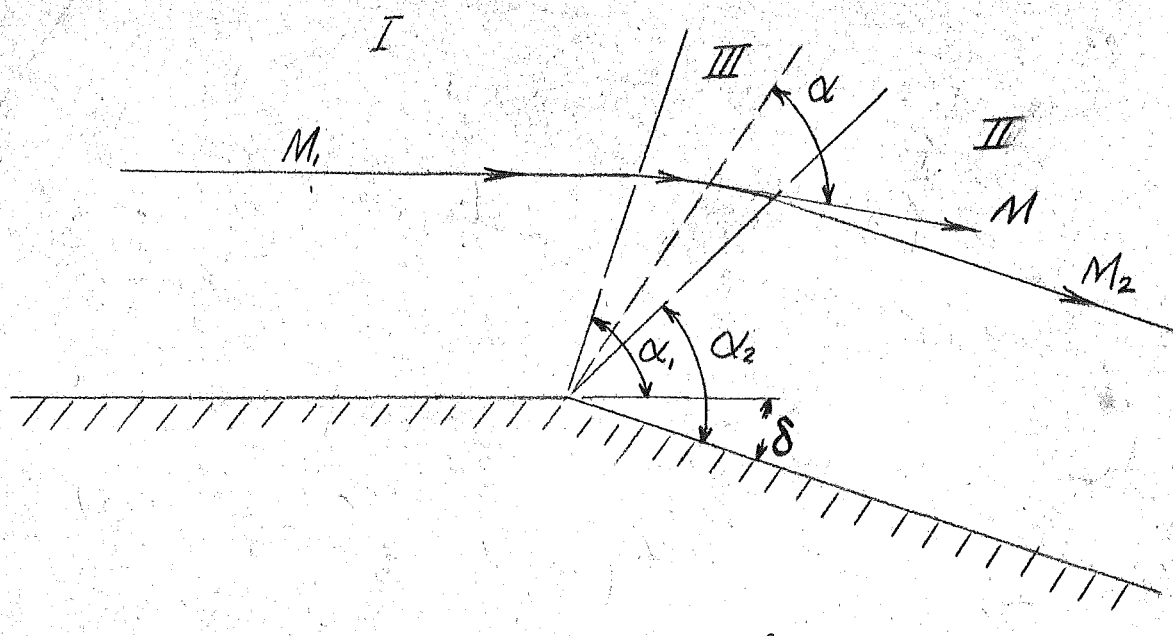

Fig. 2 Supersonic flow about a corner

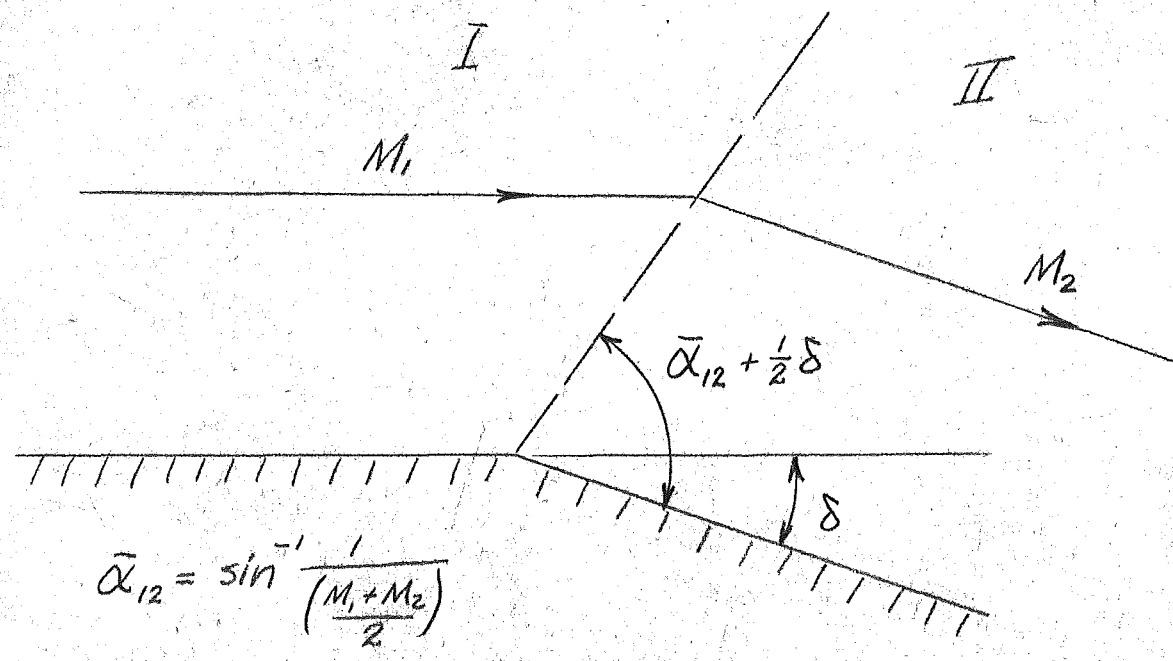

Fig. 4 Approximate representation of flow about a small corner

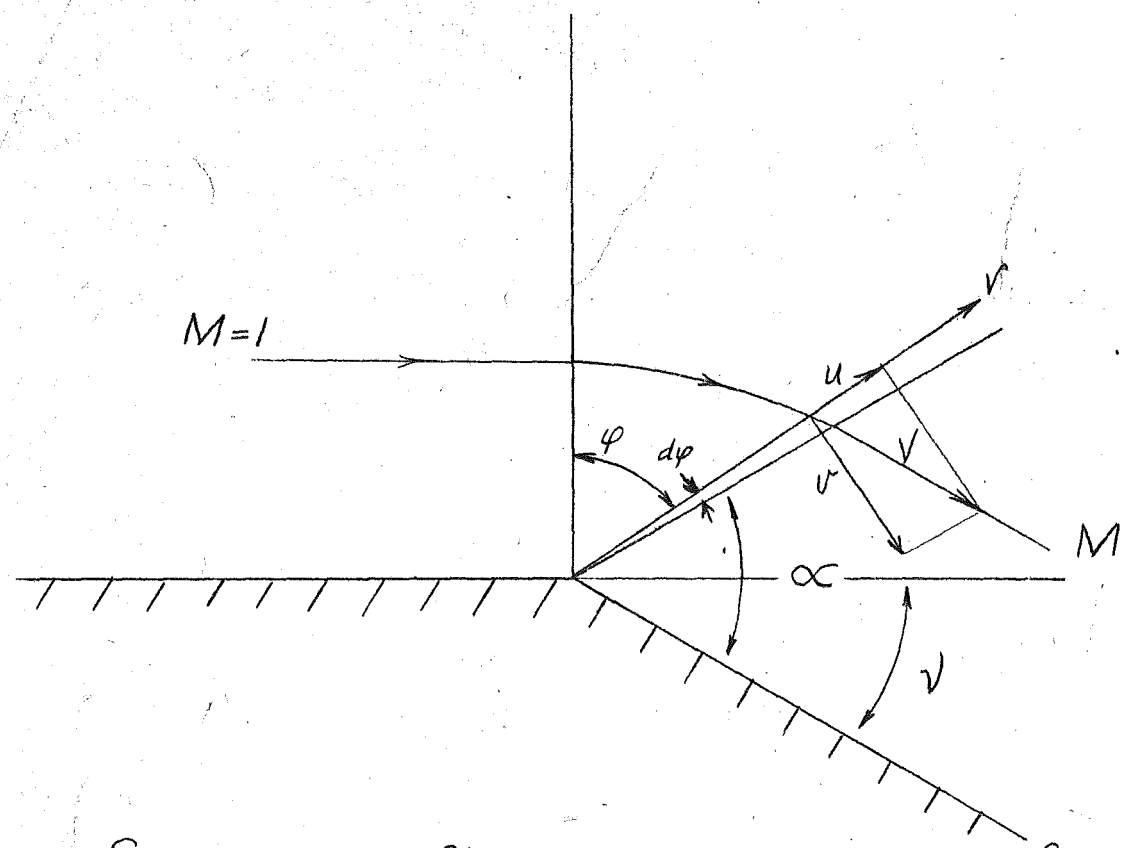

Fig. 3 Supersonic flow about a corner from an initial Mach number of unity

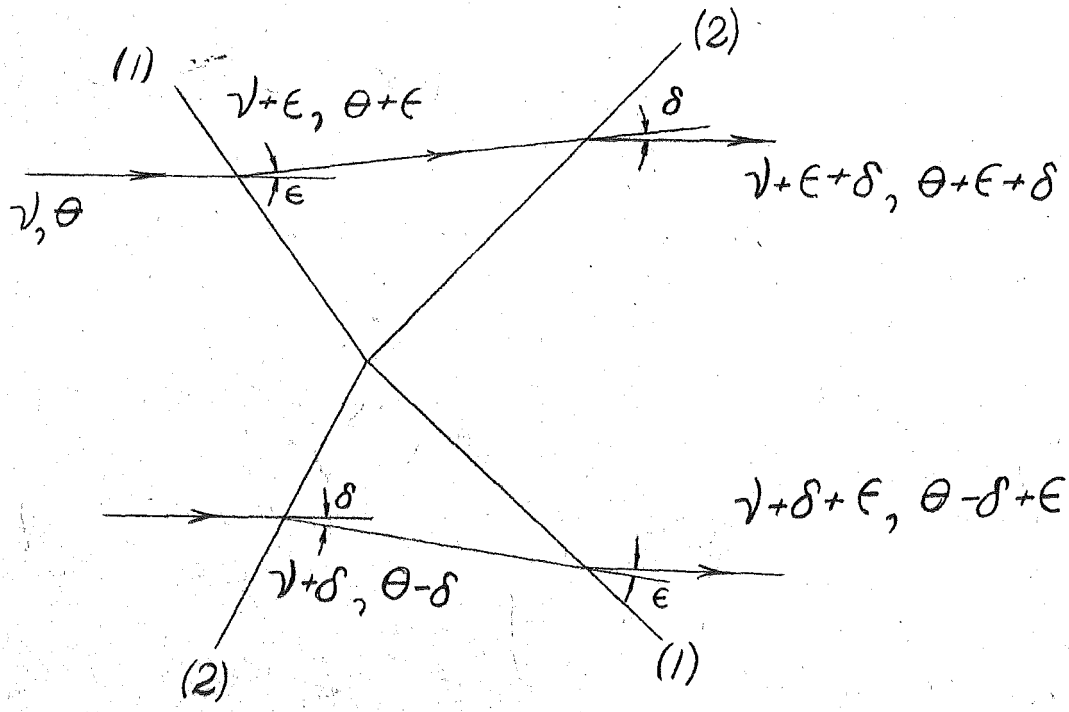

Fig. 5 Intersection of two expansion waves

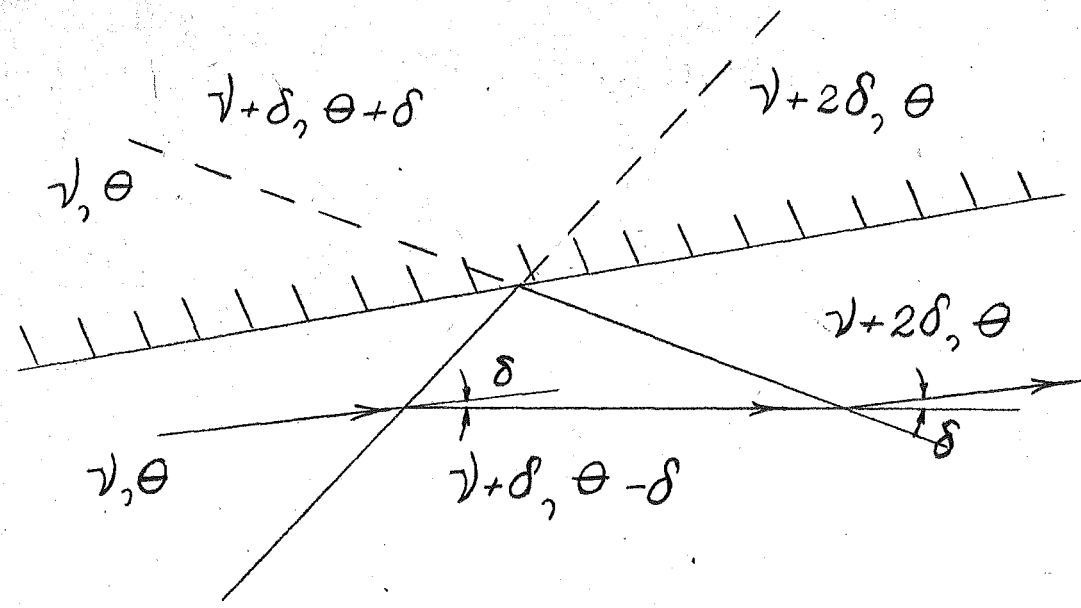

Fig. 6 Reflection of an expansion wave by a wall

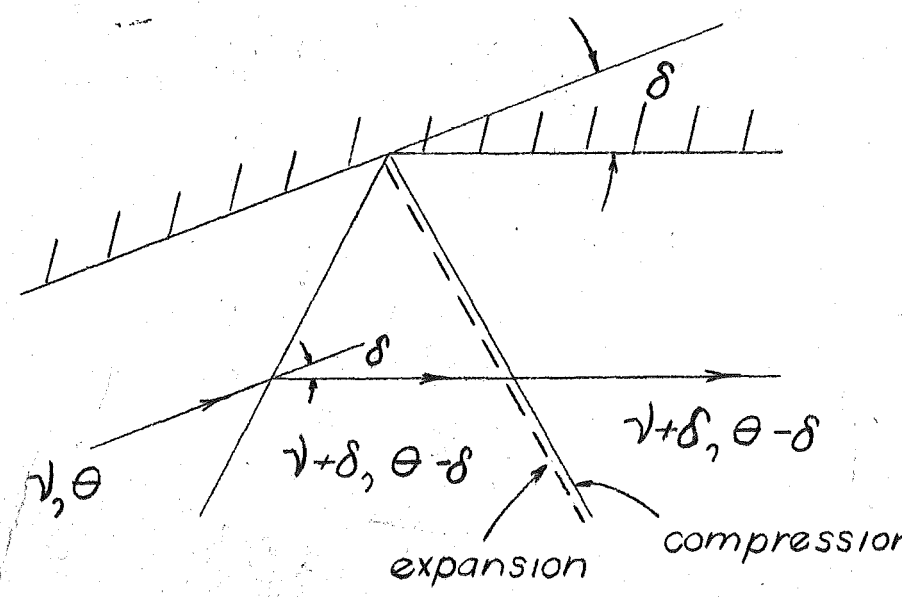

Fig. 7 Neutralization of an expansion wave

Unclassified

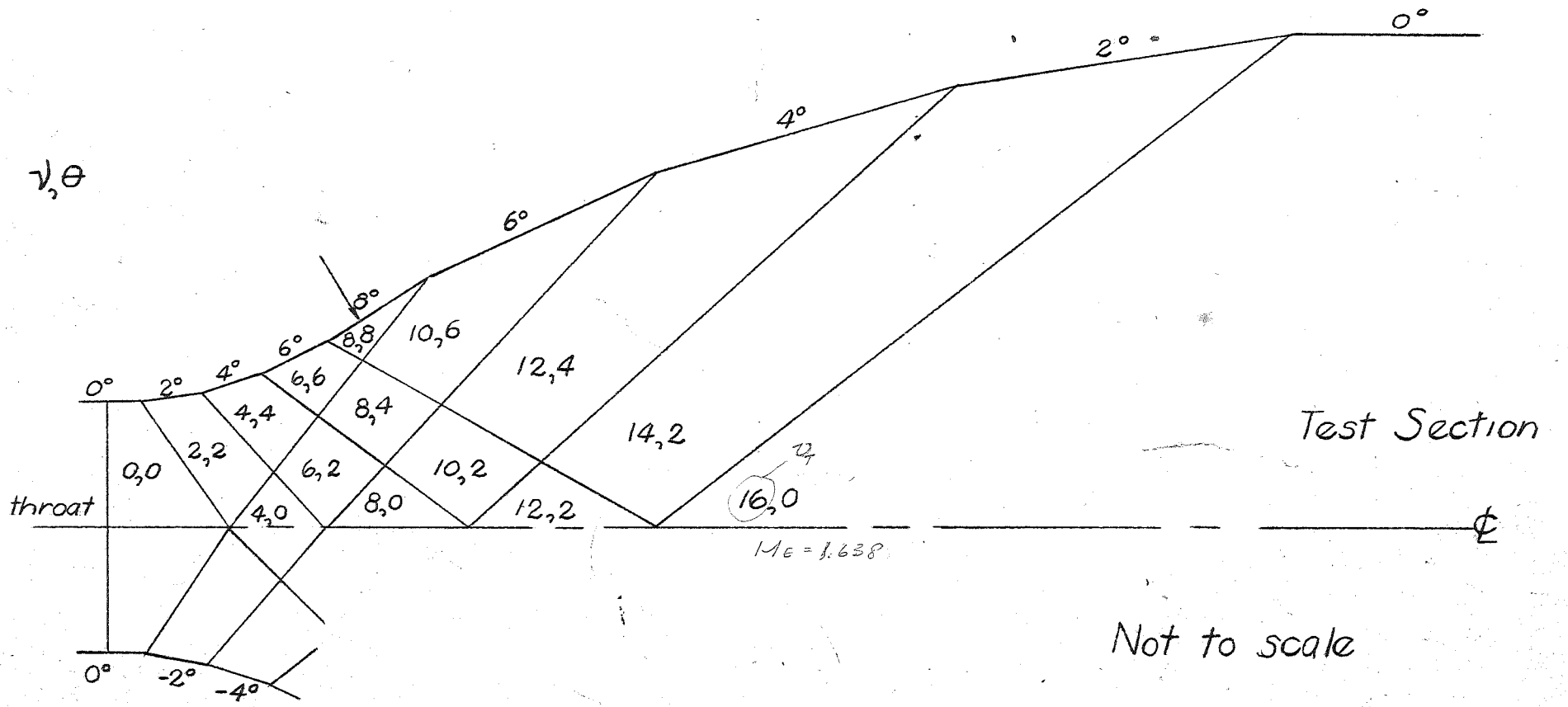

Fig. 8 Flow field in a nozzle with no reflected waves

NOLM 10594

Unclassified

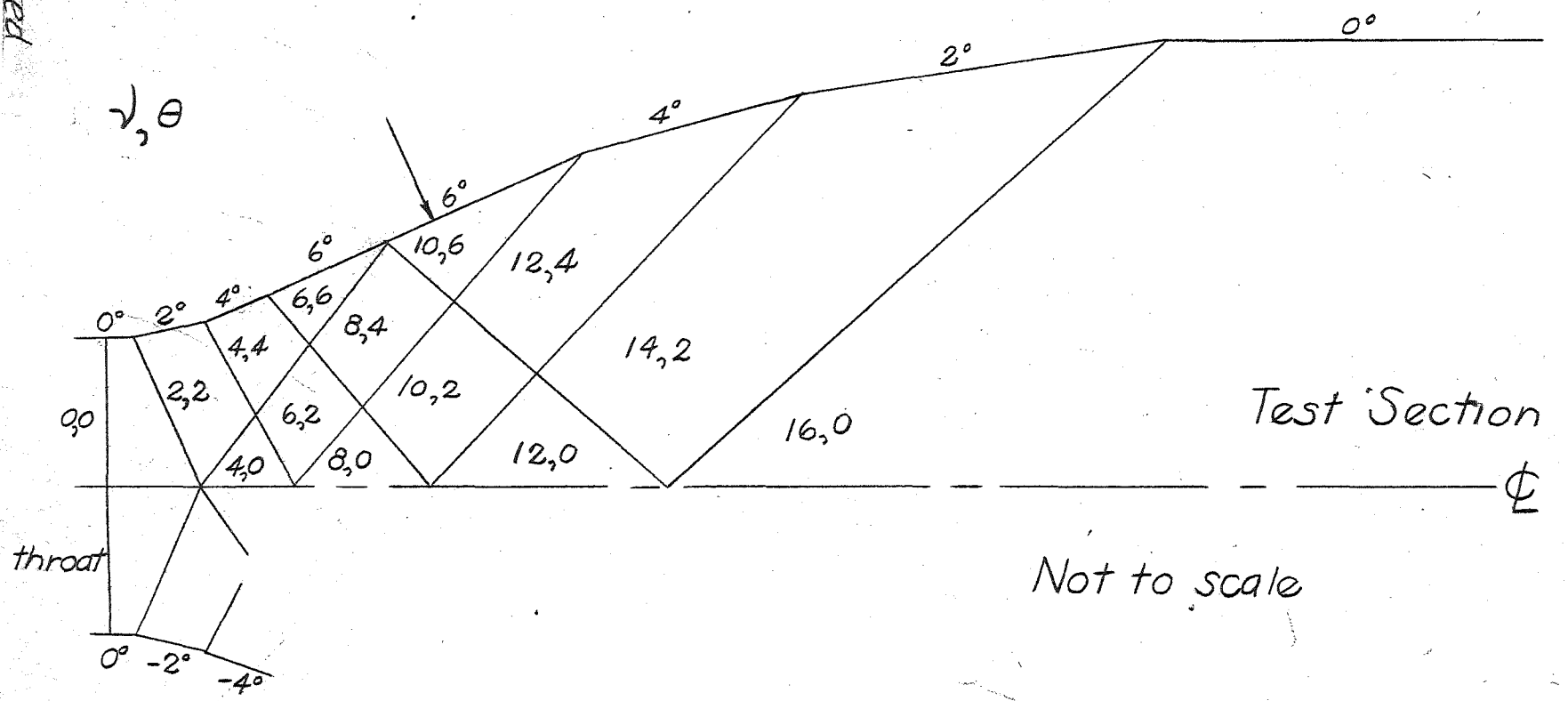

Fig. 9 Flow field in a nozzle with reflected waves

NOLM 10594

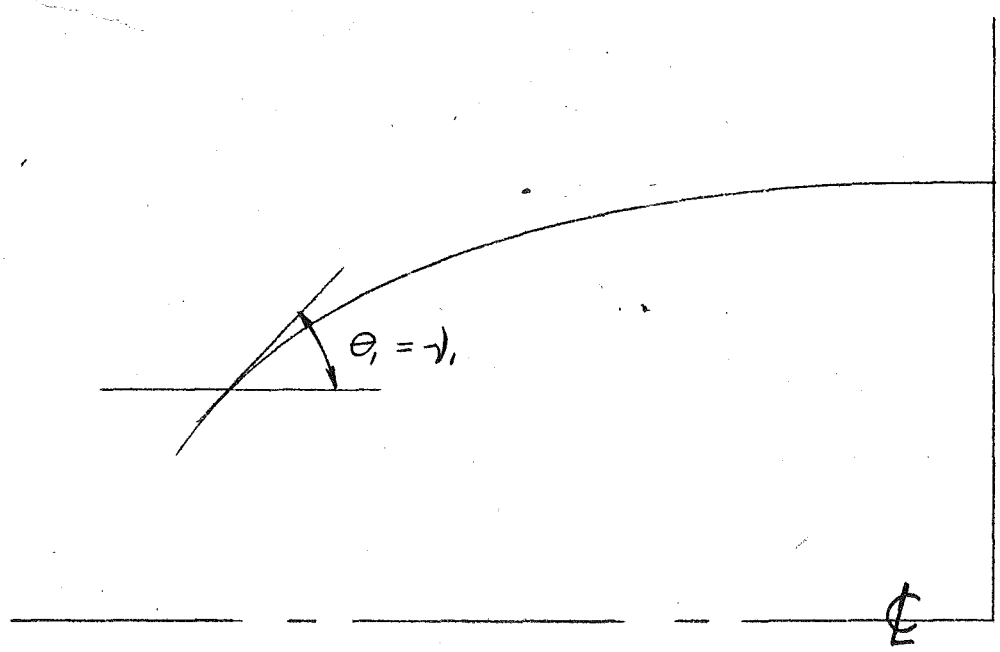

Fig. 10 Nozzle with sharp throat

Unclassified

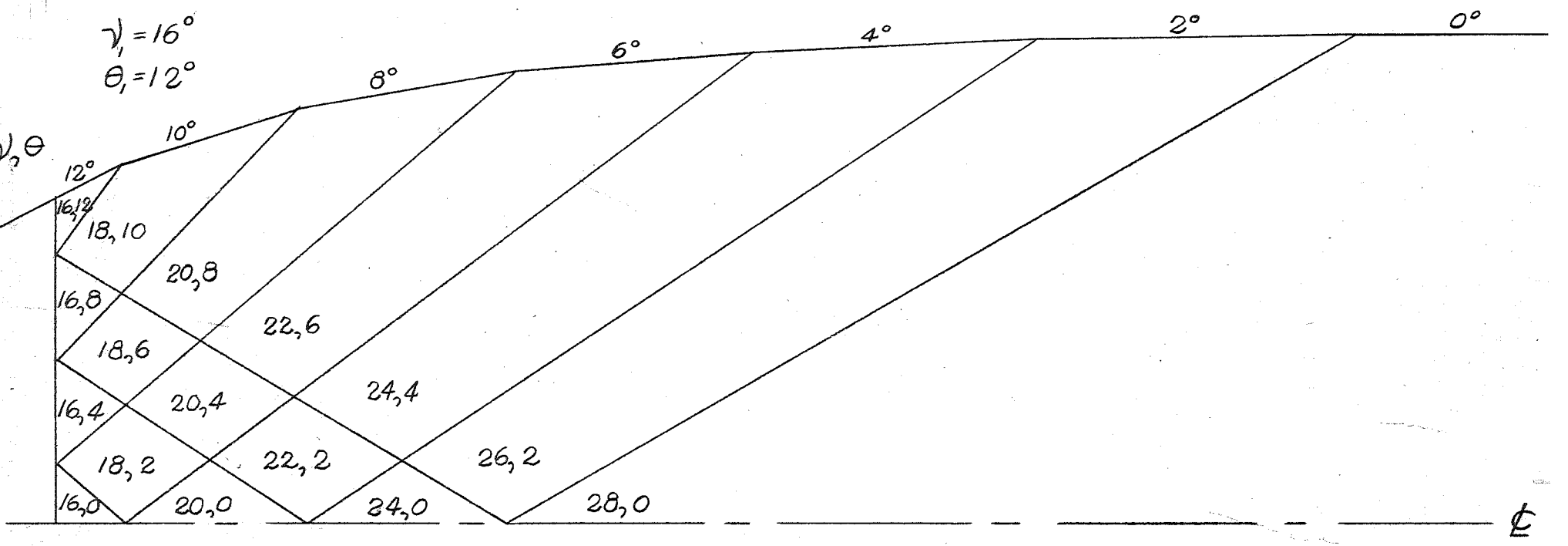

Fig. 11 Nozzle laid out according to Puckett's method (Ref. 9)

NOLM 10594

Unclassified

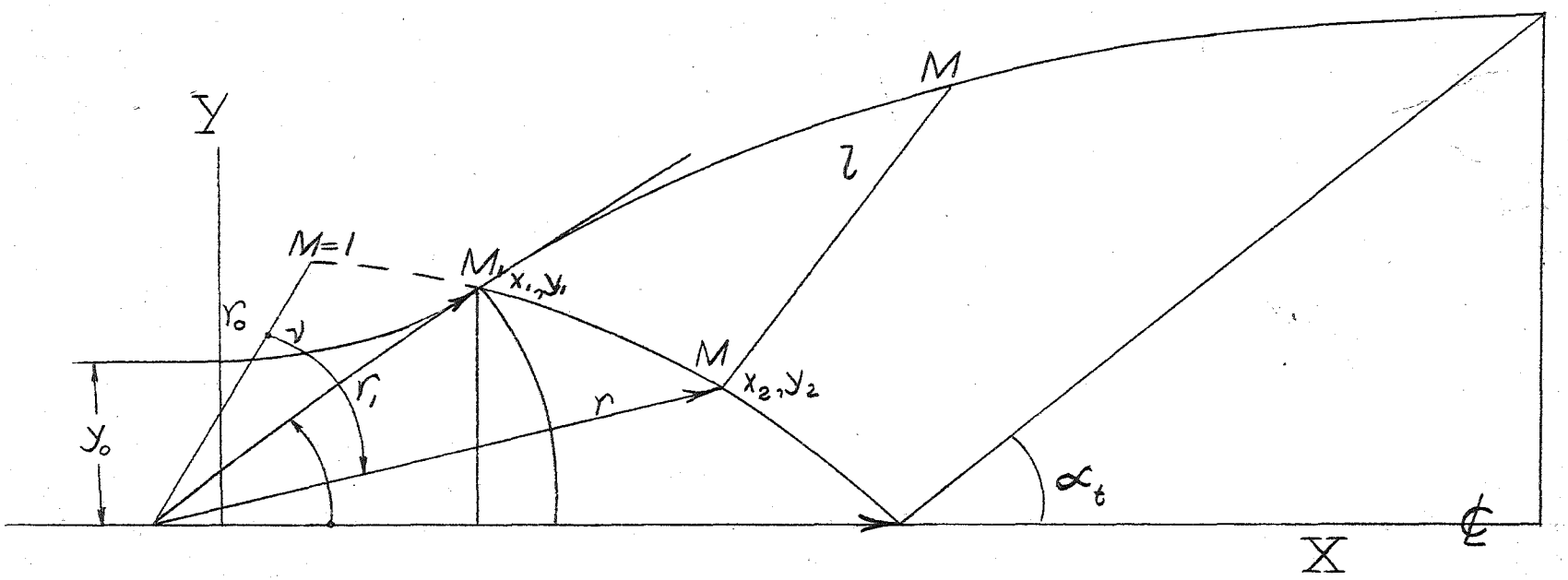

Fig. 12 Variables used with the Foelsch method (Ref. c)

NOLM 10594

Unclassified

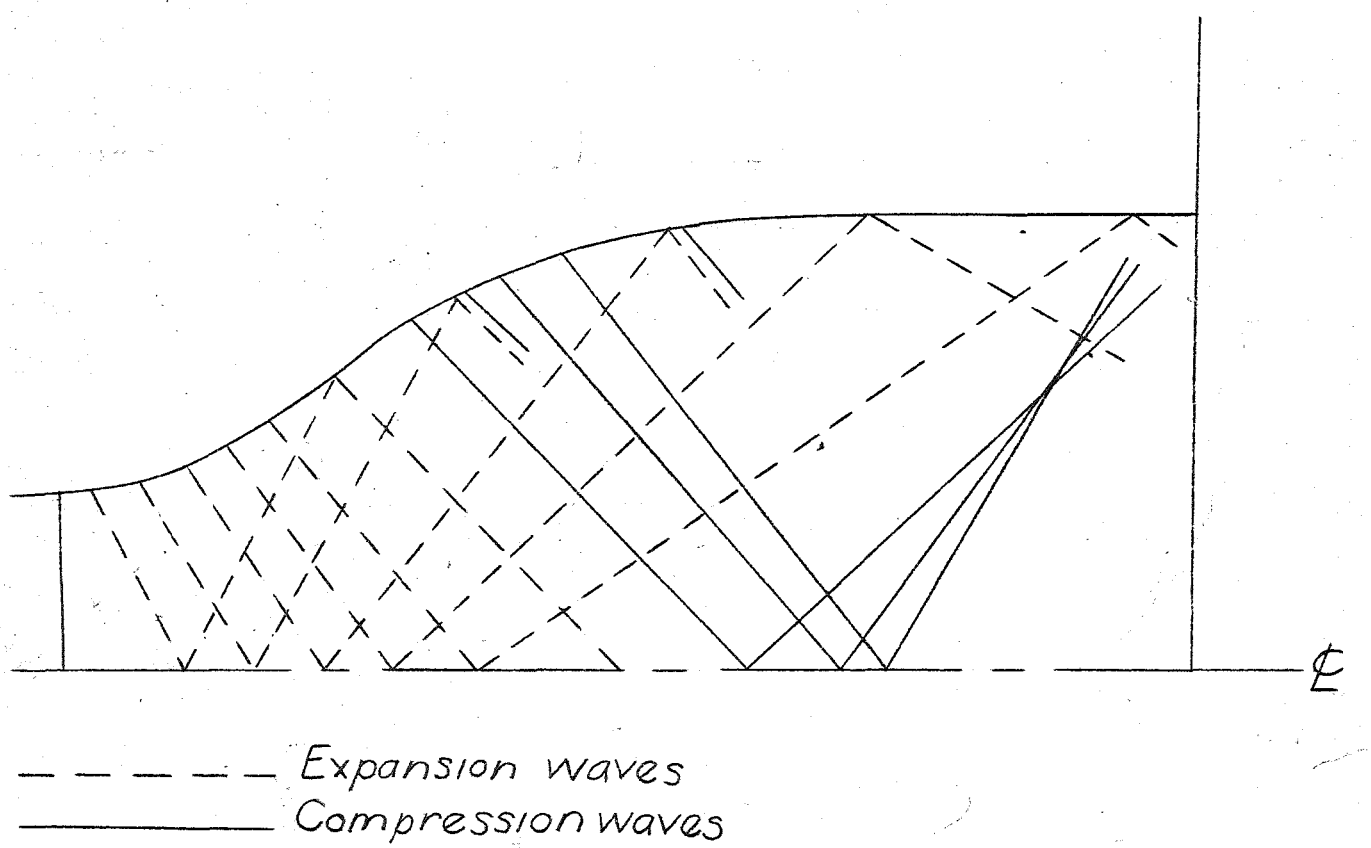

Fig. 13 Nozzle exhibiting a region of converging compression waves

NOLM 10594

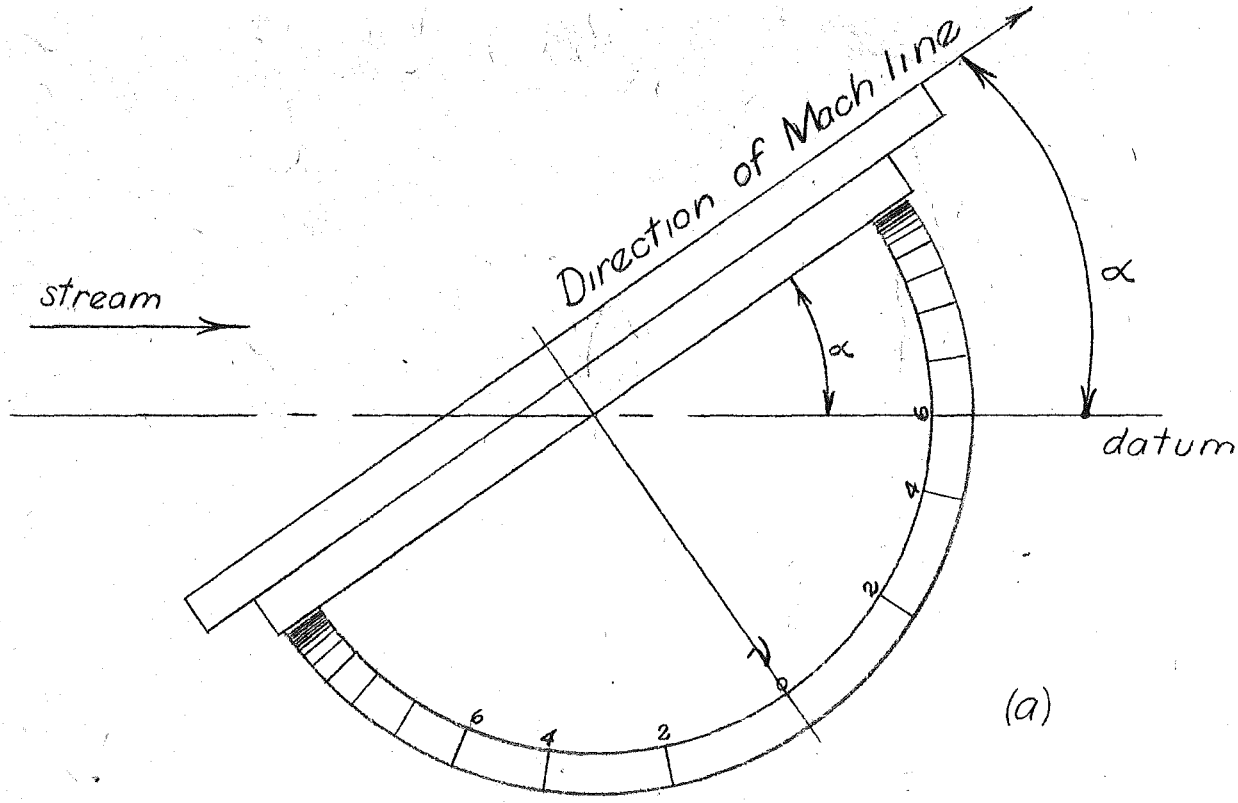

(a) Mach line directed upward in stream direction
(b) Mach line directed downward in stream direction

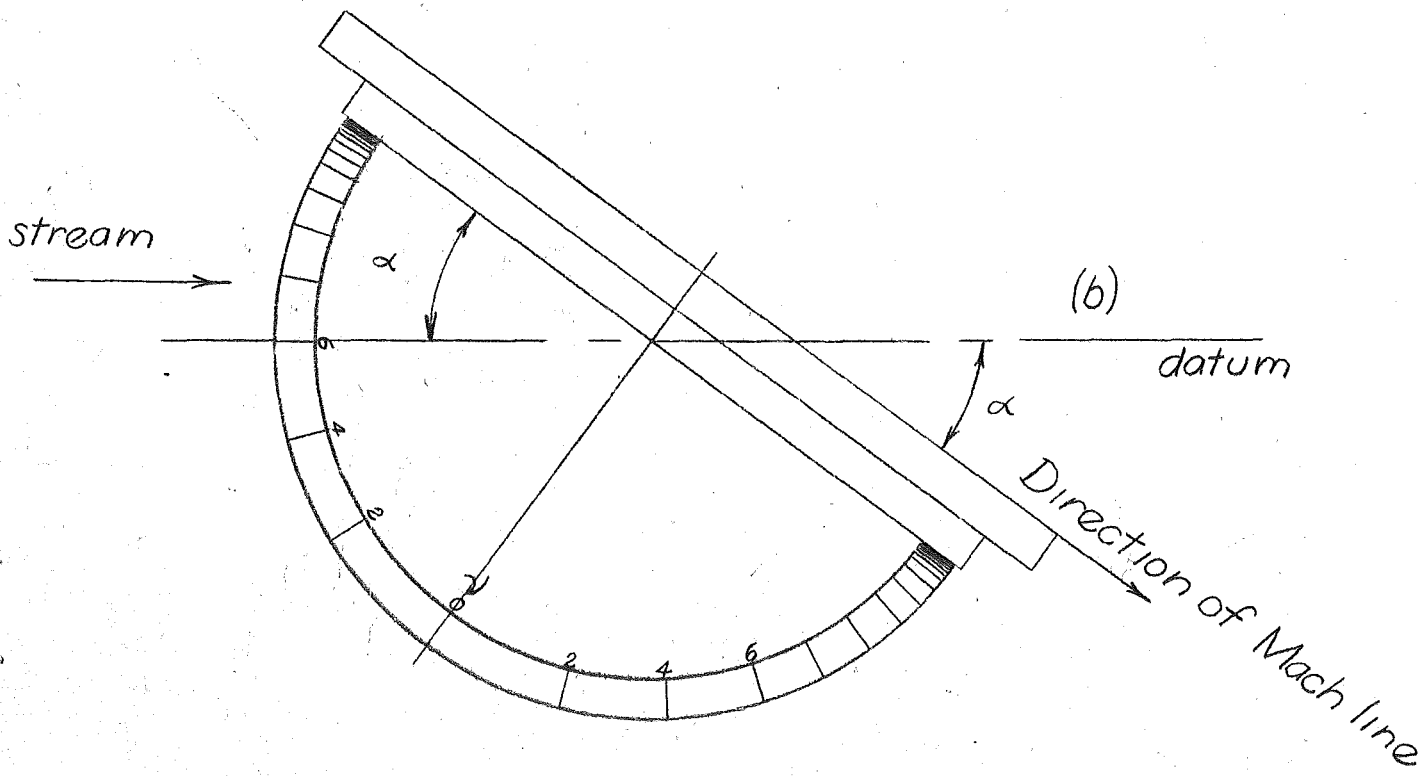

Fig. 15 Upper half of supersonic protractor NOLM 10594

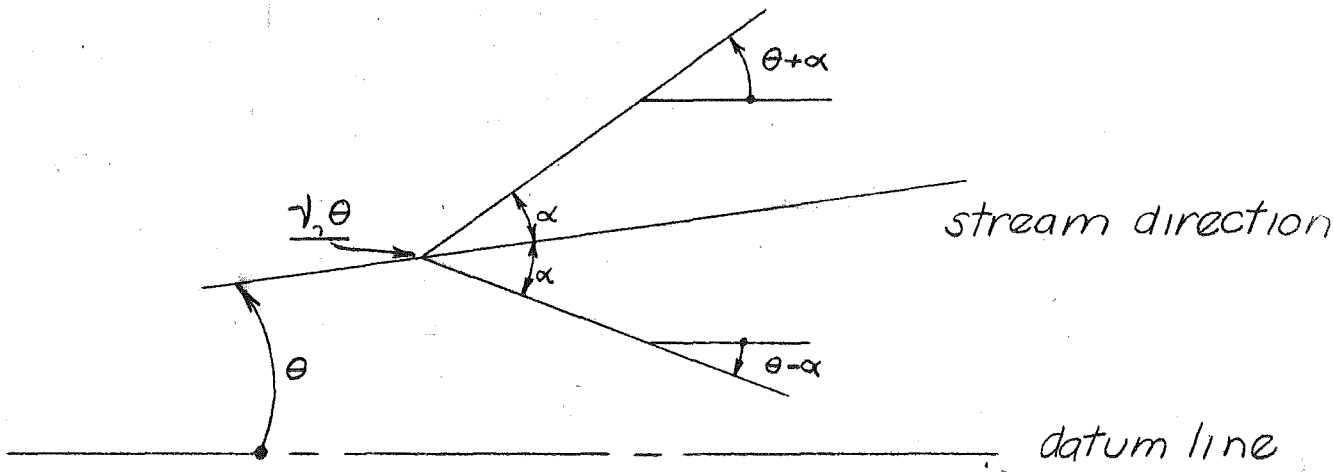

Fig. 14 Mach lines from a point disturbance

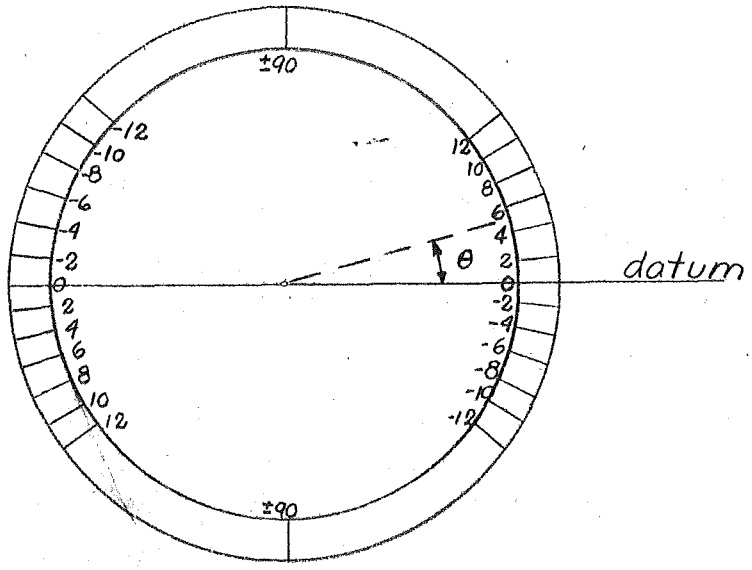

Fig. 16 Lower half of supersonic protractor

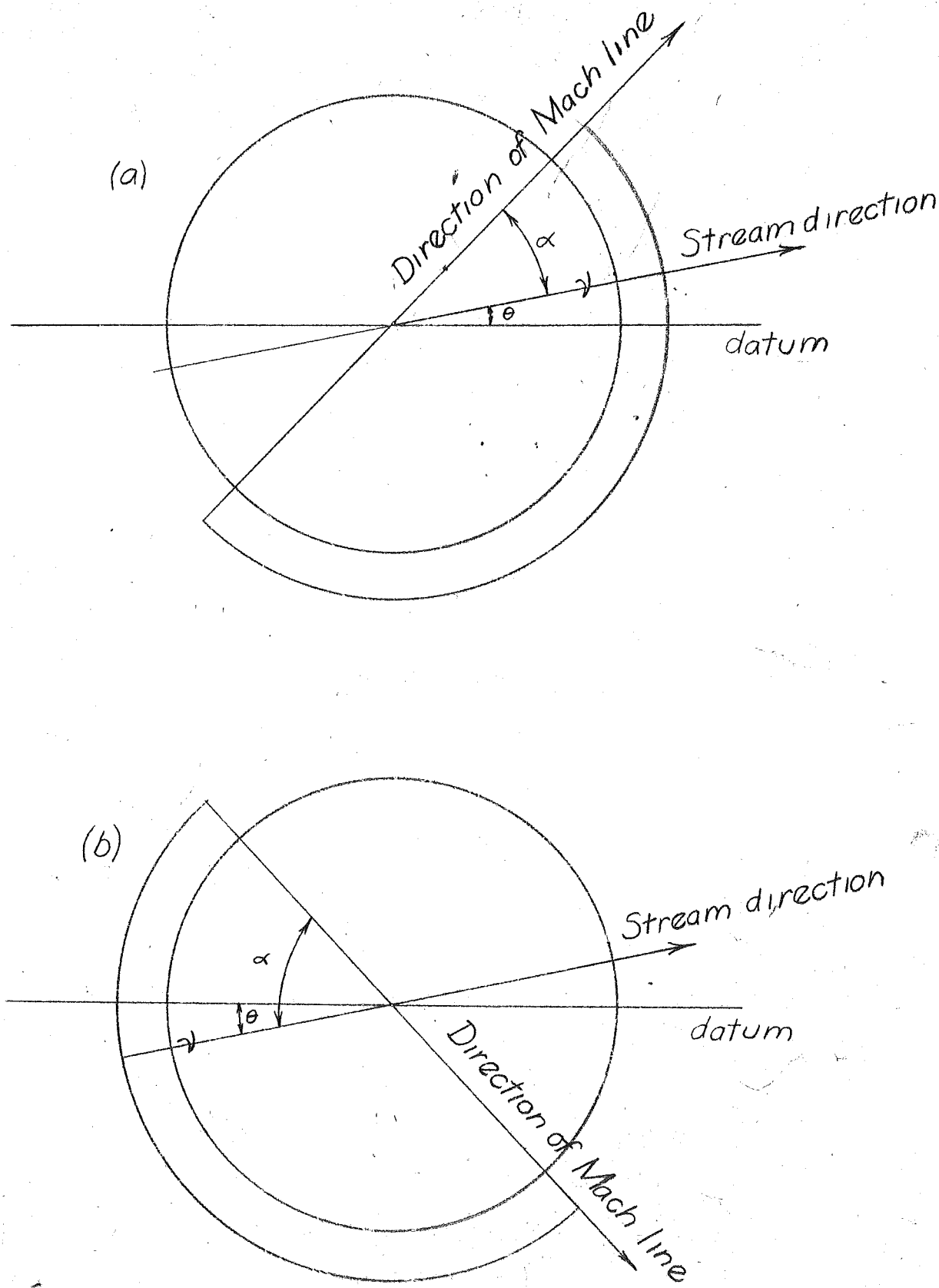

Unclassified

NOLM 10594

Fig. 17 Assembly of supersonic protractor

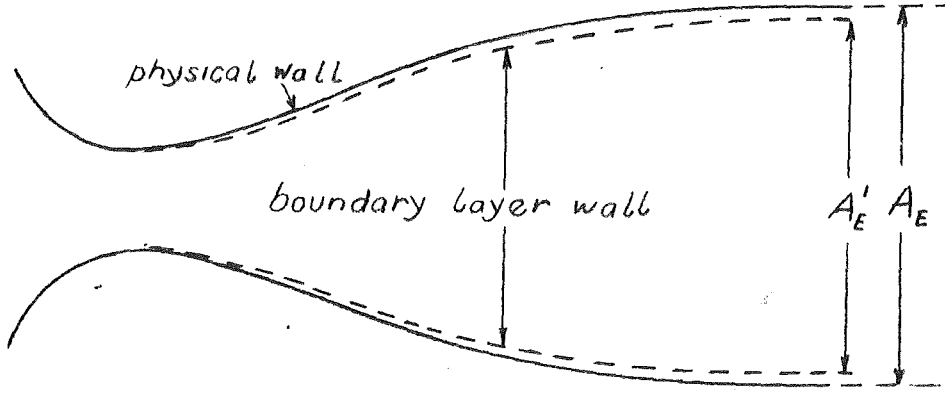

FIGURE 18. BOUNDARY LAYER WALL

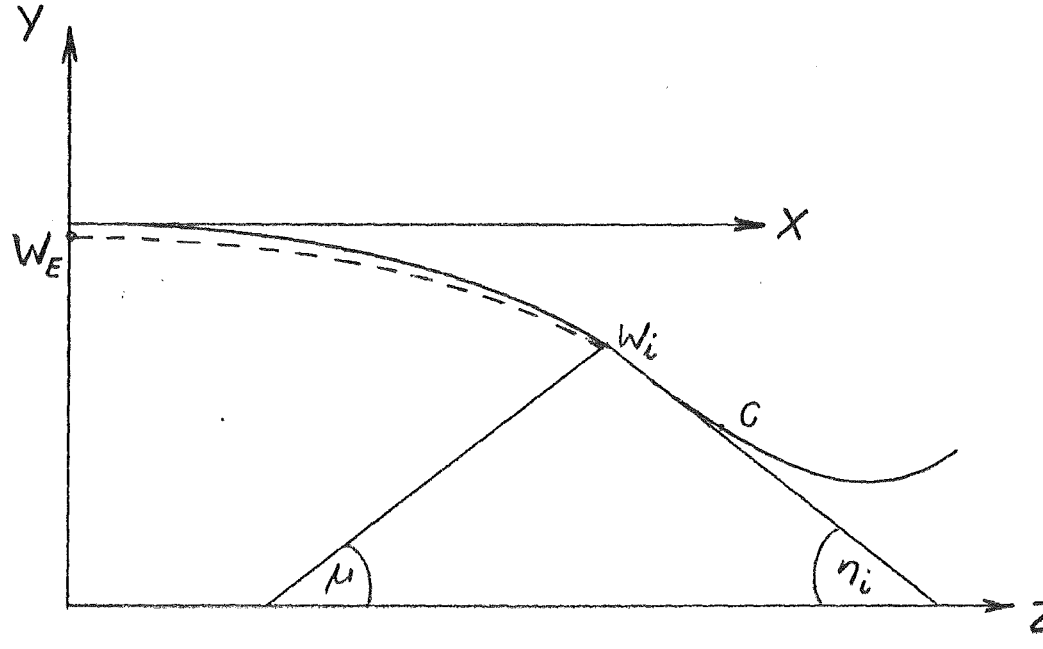

FIGURE 19. SKETCH EXPLAINING NOTATIONS

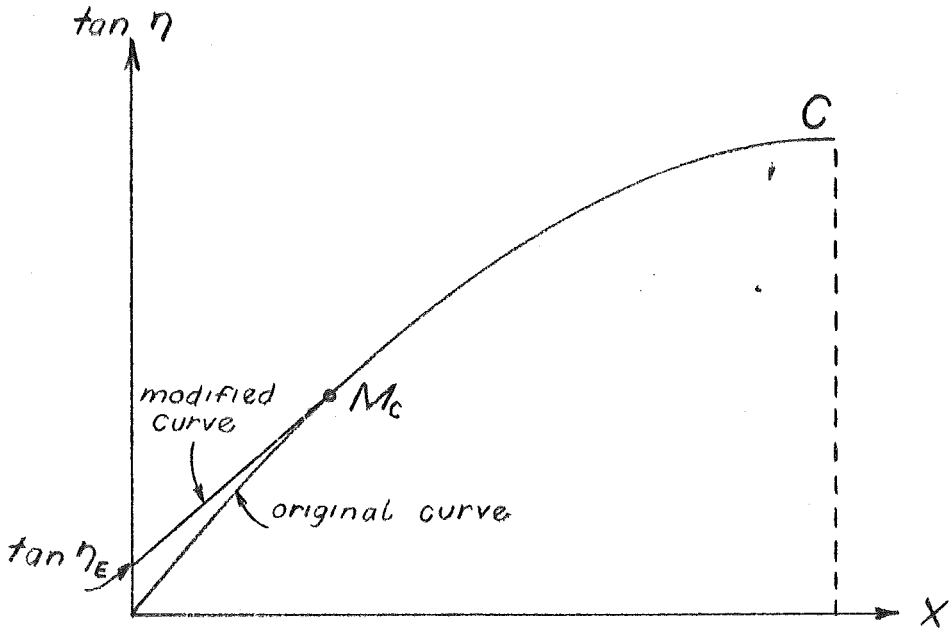

FIGURE 20. WALL SLOPE ALONG NOZZLE AXIS

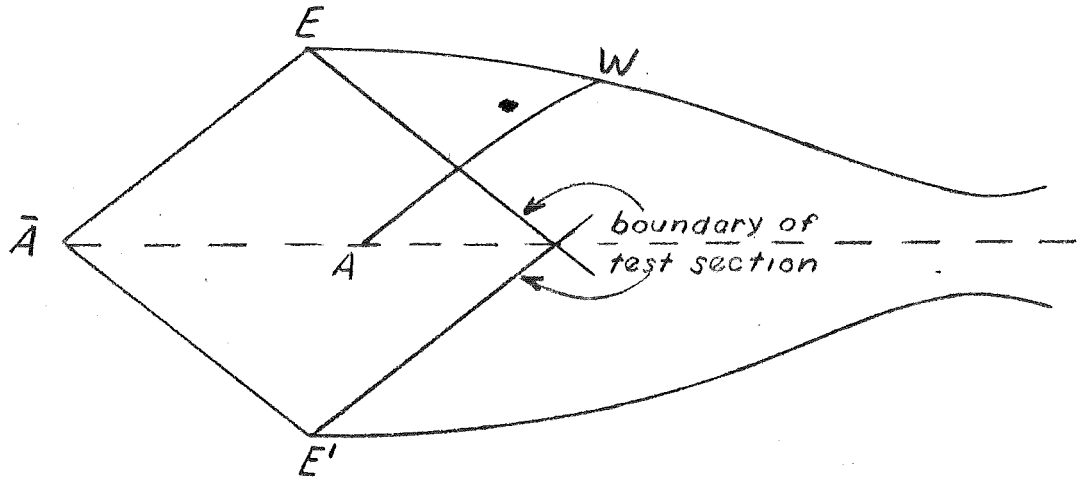

FIGURE 21. TRACING A DISTURBANCE BACK TO ITS ORIGIN

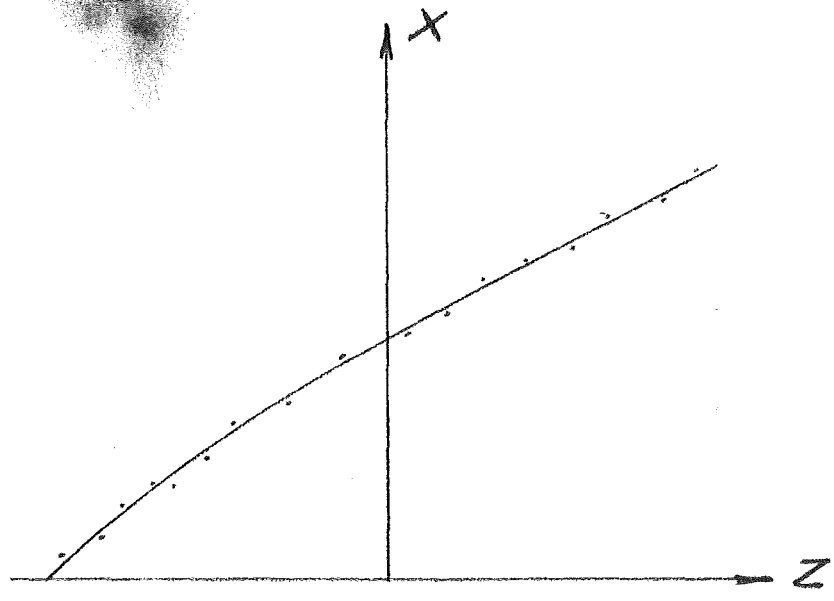

FIGURE 22. CORRELATION BETWEEN WALL AND AXIS POINTS

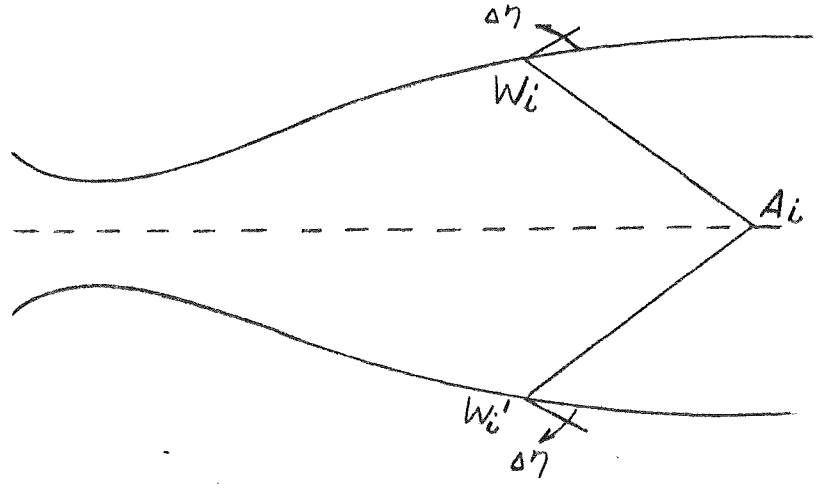

FIGURE 23. MACH LINES ORIGINATING AT ASSUMED BENDS

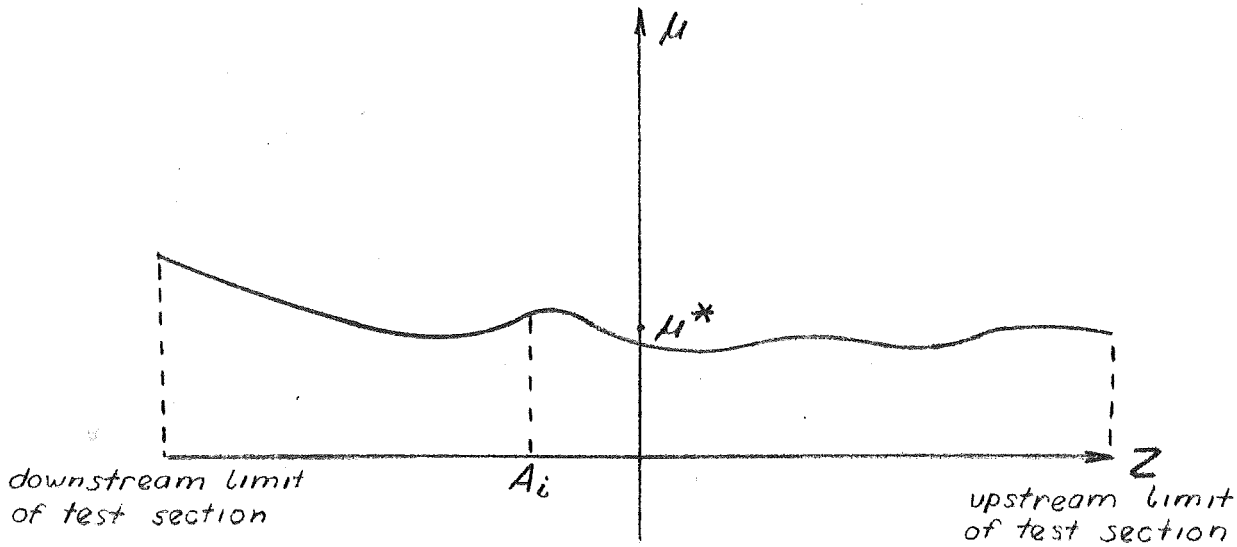

FIGURE 24. EXAMPLE OF UNSATISFATORY MACH ANGLE DISTRIBUTION

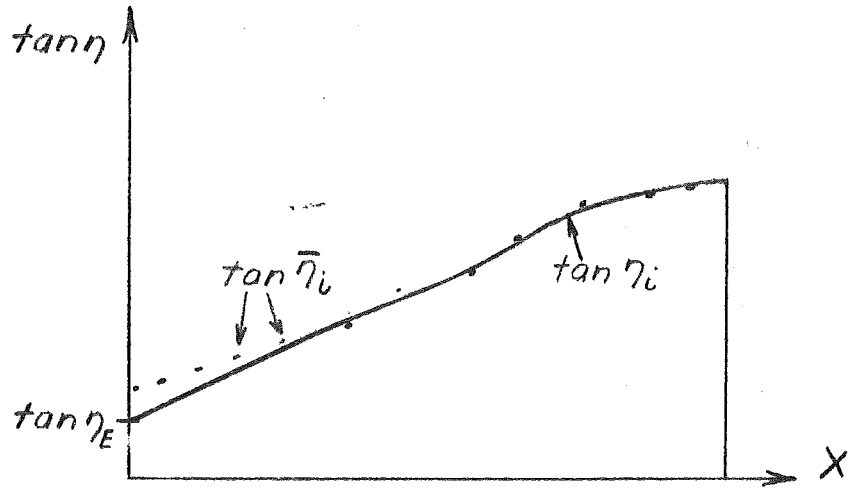

FIGURE 25. ACTUAL WALL ANGLE DISTRIBUTION AND CORRECTED ANGLES